Research Paper

GEOSPHERE

GEOSPHERE, v. 17, no. 2

https://doi.org/10.1130/GES02277.1

9 figures; 1 table; 1 set of supplemental files

CORRESPONDENCE:
steven.andrews914@gmail.com

CITATION: Andrews, S.D., Morton, A., Decou, A., and Frei, D., 2021, Reconstructing drainage pathways in the North Atlantic during the Triassic utilizing heavy minerals, mineral chemistry, and detrital zircon geochronology: Geosphere, v. 17, no. 2, p. 479–500, https://doi.org/10.1130/GES02277.1.

Science Editor: David E. Fastovsky
Associate Editor: Nancy R. Riggs

Received 21 April 2020
Revision received 23 July 2020
Accepted 5 January 2021

Published online 25 February 2021

Reconstructing drainage pathways in the North Atlantic during the Triassic utilizing heavy minerals, mineral chemistry, and detrital zircon geochronology

Steven D. Andrews[1,2], Andrew Morton[2,3], Audrey Decou[1], and Dirk Frei[4]

[1]University of the Highlands and Islands, Inverness IV2 5NA, UK
[2]CASP, West Building, Madingley Rise, Madingley Road, Cambridge CB3 0UD, UK
[3]HM Research Associates Ltd., Giddanmu, St. Ishmaels SA62 3TJ, UK
[4]Department of Earth Sciences, University of the Western Cape, Bellville 7530, South Africa

ABSTRACT

In this study, single-grain mineral geochemistry, detrital zircon geochronology, and conventional heavy-mineral analysis are used to elucidate sediment transport pathways that existed in the North Atlantic region during the Triassic. The presence of lateral and axial drainage systems is identified and their source regions are constrained.

Axial systems are suggested to have likely delivered sediment sourced in East Greenland (Milne Land–Renland) as far south as the south Viking Graben (>800 km). Furthermore, the data highlight the existence of lateral systems issuing from Western Norway and the Shetland Platform as well as a major east-west–aligned drainage divide positioned adjacent to the Milne Land–Renland region. This divide separated the catchments that flowed north to the Boreal Ocean from those that flowed south into a series of endoreic basins and, ultimately, the Tethys Sea. A further potential drainage divide is identified to the west of Shetland.

The data presented and the conclusions reached have major implications for reservoir prediction, as well as correlation, throughout the region. Furthermore, understanding the drainage networks that existed during the Triassic can help constrain paleogeographic reconstructions and provides an important framework for the construction of facies models in the region.

INTRODUCTION

The Triassic basins of the North Atlantic record the initial phases of rifting, which eventually led to the breakup of Pangea (Manspeizer, 1988; Leleu et al., 2016). The intracontinental nature of this rift system resulted in the predominance of fluvial, lacustrine, and aeolian sedimentary systems that formed thick continental successions. Much previous work has focused on the stratigraphy and sedimentology of individual basins, and a number of studies have investigated provenance relationships in individual regions, as summarized by McKie and Williams (2009). However, the scale of the rift system provides an ideal setting for an integrated investigation into how these basins were linked by large-scale drainage networks. Understanding these drainage networks can shed light on how the rift evolved and is key for reservoir prediction. Furthermore, understanding the drainage networks that existed during the Triassic provides an important framework within which facies models and paleogeographic reconstructions for the region can be constrained. The provenance data presented here also aid in regional correlation.

This study integrates conventional heavy-mineral analysis (187 samples), single-grain mineral geochemistry (42 garnet and 23 rutile analyses) and detrital zircon geochronology data sets (17 samples) acquired from Triassic sandstones in the northern North Sea, west of Shetland, and the Norwegian Sea areas. All heavy mineral data used in this study are available in the Supplemental Material[1]. The ultimate aim of the study is to constrain sediment sources and in particular to assess the role of East Greenland as a provider of detritus.

Ten wells were selected from across the region (Fig. 1), covering much of the Triassic stratigraphy (Figs. 2 and 3): UK well 164/25-1ST, in the northern Rockall Trough; UK wells 205/26a-3, 205/26a-4, and 204/30-2, Strathmore Field, west of Shetland (including data from Morton et al., 2007); UK well 220/26-2, at the northern end of the Shetland Platform; Norwegian well 6/3-1, toward the southern end of the Viking Graben; Norwegian well 31/6-1, in the northern part of the Viking Graben adjacent to the Norwegian landmass; Norwegian well 6201/11-1, in the southern Møre Basin; and Norwegian wells 6507/6-1 and 6608/8-1 from the Nordland Ridge in the Norwegian Sea (Fig. 1).

STRATIGRAPHIC FRAMEWORK

Considerable challenges exist when working on the Triassic of the North Atlantic on a regional scale. Correlation is often problematic due to poor biostratigraphic constraints and regionally variable lithostratigraphy. The stratigraphic determinations and correlations made here (Fig. 3) are based on

Steven Andrews https://orcid.org/0000-0002-0418-0809

Goldsmith et al. (2003), McKie and Williams (2009), and original interpretations of wireline data alongside completion logs. The Norwegian lithostratigraphic nomenclature (Lervik, 2006) has been used where possible, due to its greater regional consistency. A composite section from the Jameson Land Basin (East Greenland) is included in the well correlations to fill the data gap that exists between the northern North Sea and Mid-Norway and to allow tentative correlation between these two regions.

GEOLOGICAL BACKGROUND

Basin formation in the North Atlantic region was initiated in the Devonian (Stemmerik et al., 1991) as a result of the collapse of the Caledonian orogen (McClay et al., 1986; Surlyk, 1990). The sedimentary rift basins on the conjugate continental margins of Norway and Greenland and the adjacent North Sea developed as a result of a series of post–Late Permian rift episodes until the Early Cenozoic, when complete continental separation took place (Surlyk et al., 1986; Stemmerik et al., 1991; Price et al., 1997; Whitham et al., 1999). Basins containing up to 8 km of Triassic fill have been reported (Doré, 1992). During the Triassic, the North Atlantic region was positioned in the northern arid belt, and deposition largely took place in dryland continental settings (McKie, 2014). Red bed sandstones and mudstones were deposited in a range of environments, including large perennial rivers and more ephemeral systems associated with aeolian, playa, lacustrine, marginal marine, and evaporite facies (McKie and Williams, 2009). Triassic sandstones from the northern North Sea and Mid-Norway Continental Shelf have proved to be major hydrocarbon reservoirs, usually in tilted fault blocks (Fisher and Mudge, 1998; McKie, 2014).

ANALYTICAL METHODS

Sample Preparation

Core samples were disaggregated, immersed in water, and cleaned by ultrasonic probe to remove and disperse any clay adhering to grain surfaces. It was not necessary to disaggregate cuttings samples since these are already broken down by the action of the drill bit. The disaggregated samples were washed through a 63 µm sieve and resubjected to ultrasonic treatment until no more clay passed into suspension, followed by wet sieving through the 125 and 63 µm sieves. The resulting >125 µm and 63–125 µm fractions were dried in an oven at 80 °C. The 63–125 µm fractions were placed in bromoform with a measured specific gravity of 2.8. Heavy minerals were allowed to separate under gravity, with frequent stirring to ensure complete separation. Heavy-mineral residues were mounted under Canada balsam for optical study using a polarizing microscope, with additional separates retained for single-grain analytical work.

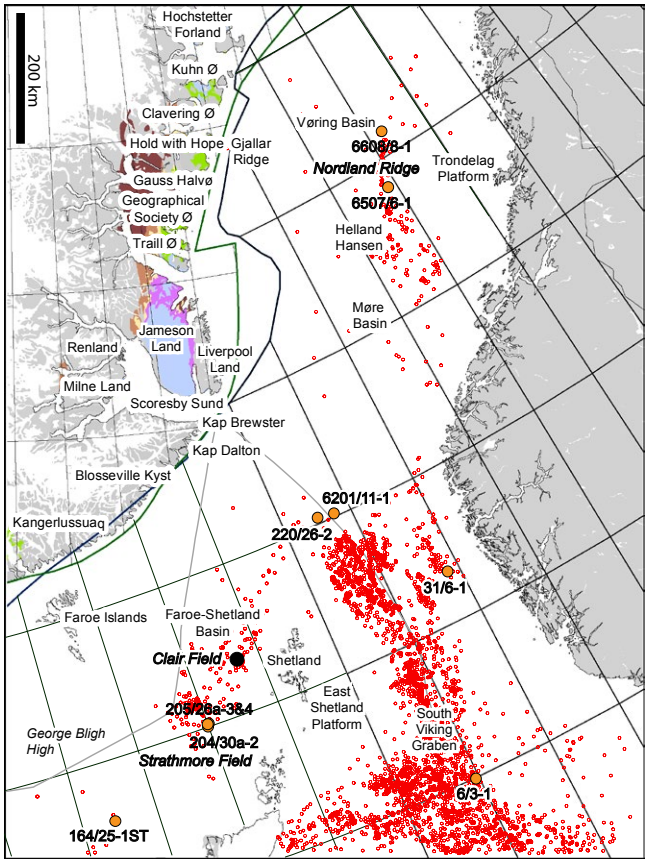

Figure 1. Map of the Norway-Greenland Sea region, prior to the onset of sea floor spreading in the Paleogene, showing the distribution of studied wells from Mid Norway, the North Sea, and the West of Shetland. Reconstruction based on the best-fit prior to final opening of the North Atlantic (magnetic anomaly 24).

Conventional (Petrographic) Heavy-Mineral Analysis

Heavy-mineral proportions were estimated by counting 200 non-opaque detrital grains using the ribbon method described by Galehouse (1971). Identification was made on the basis of optical properties, as described for grain mounts by Mange and Maurer (1992). Provenance-sensitive mineral ratios

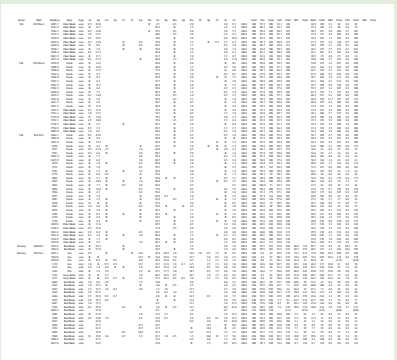

[1]Supplemental Material. Heavy mineral datasets. Please visit https://doi.org/10.1130/GEOS.S.13524584 to access the supplemental material, and contact editing@geosociety.org with any questions.

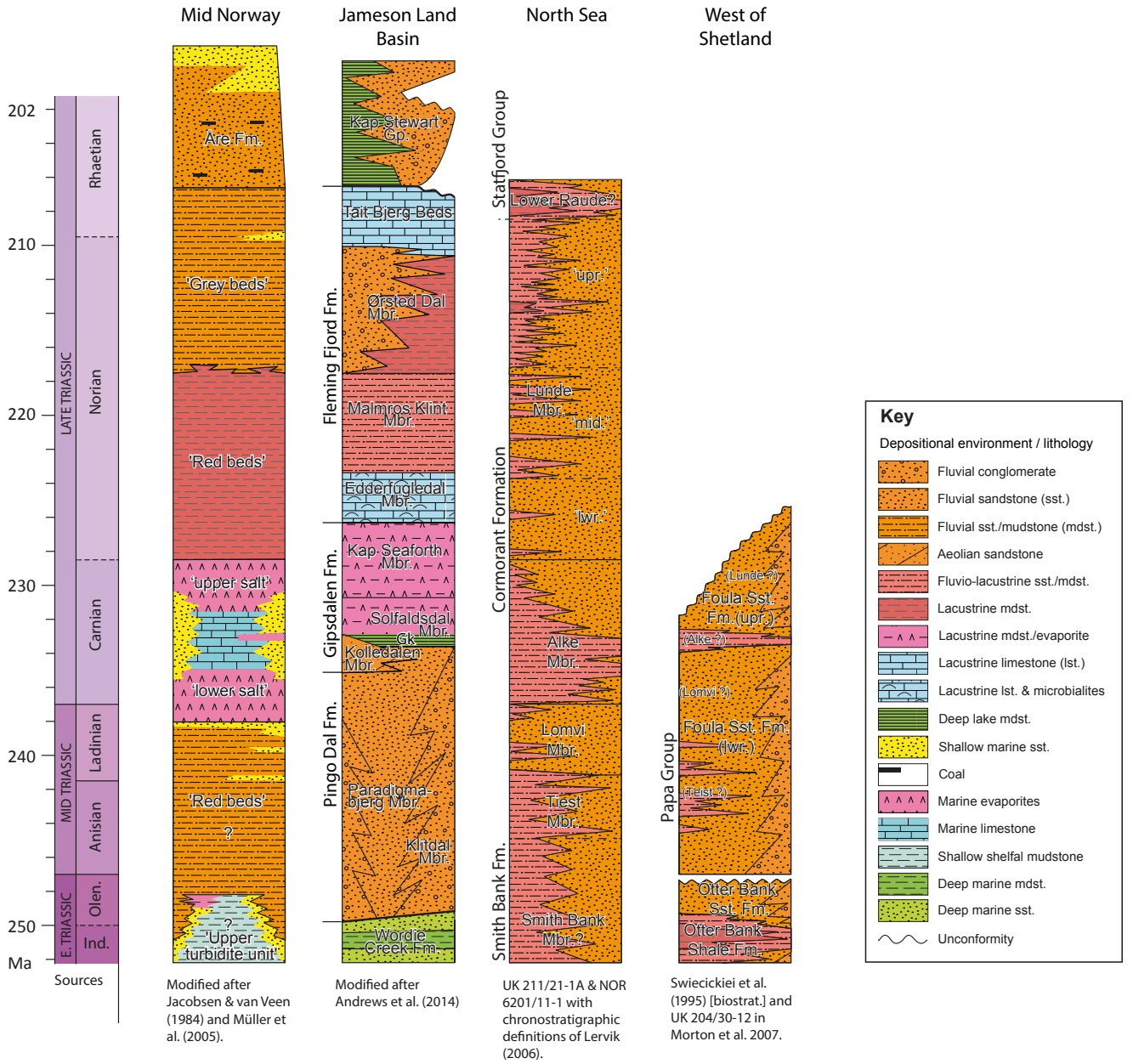

Figure 2. Triassic stratigraphy of the study area: Mid Norway, East Greenland (Jameson Land Basin), The North Sea, and West of Shetland.

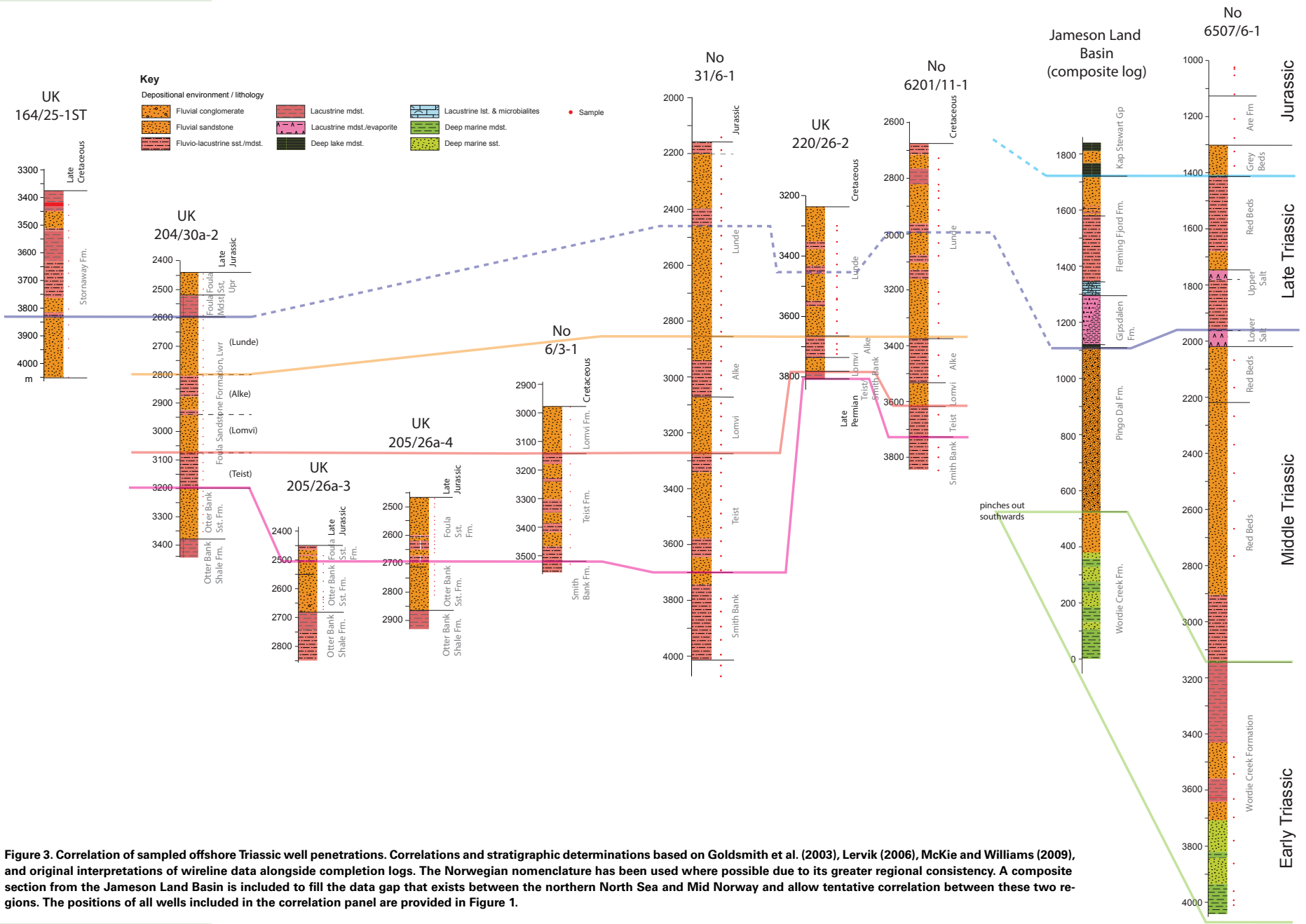

Figure 3. Correlation of sampled offshore Triassic well penetrations. Correlations and stratigraphic determinations based on Goldsmith et al. (2003), Lervik (2006), McKie and Williams (2009), and original interpretations of wireline data alongside completion logs. The Norwegian nomenclature has been used where possible due to its greater regional consistency. A composite section from the Jameson Land Basin is included to fill the data gap that exists between the northern North Sea and Mid Norway and allow tentative correlation between these two regions. The positions of all wells included in the correlation panel are provided in Figure 1.

(Morton and Hallsworth, 1994) were also determined using the ribbon counting method. Previous studies of the Triassic in the central North Sea have revealed the importance of heavy-mineral grain textures for stratigraphic analysis and provenance interpretations (Mange-Rajetzky, 1995). Variations in tourmaline, zircon, and apatite morphology were considered by Mange-Rajetzky (1995) to have greater stratigraphic value than heavy-mineral abundances in this region. In recent studies of the central North Sea Triassic, apatite morphology, and in particular the apatite roundness index (ARi), has proved to be a reliable and stratigraphically significant textural measurement (Mouritzen et al., 2017), and hence this index has been determined for the new wells analyzed in the course of this study. ARi is determined as % rounded apatite in the total apatite population, following Morton et al. (2010).

Garnet Geochemistry

Garnet major-element mineral chemistry was undertaken by electron microprobe analysis (EMPA) following the method originally described by Morton (1985). Grains were extracted from heavy-mineral separates during optical examination under the polarizing microscope and analyzed at Aberdeen University using a Link Systems AN10000 energy-dispersive X-ray analyzer attached to a Cambridge Instruments Microscan V electron microprobe. The quality of each result was monitored to ensure that the stoichiometrically determined formulae corresponded to ideal garnet compositions. Fifty single-grain analyses were made per sample. Garnet compositions are expressed in terms of the relative abundance of the Mg, Fe^{2+}, Ca, and Mn end members. The compositions of garnet assemblages were plotted on ternary diagrams with proportions of Fe^{2+}+Mn, Mg, and Ca in the garnet formula as poles, calculated assuming all Fe is present as Fe^{2+}. Relative proportions of Types A, B, and C garnets (Morton et al., 2004; Mange and Morton, 2007) are shown as pie charts to aid clarity.

Rutile Geochemistry

Rutile trace-element geochemistry was carried out by laser ablation–inductively coupled plasma mass spectrometry (LA-ICP-MS). Samples were selected on the basis of the results of the conventional optical analysis. Grains were extracted from heavy-mineral separates during optical examination under the polarizing microscope and analyzed either in the School of Earth, Ocean and Planetary Sciences at Cardiff University, UK, or at the Central Analytical Facility (CAF), Stellenbosch University, South Africa.

The analysis at Cardiff was carried out by a Thermo Elemental X(7) series ICP-MS coupled to a New Wave Research UP213 Nd:YAG 213 nm UV laser. Laser beam diameter was 30 µm, and laser repetition rate was set at 4 Hz. Helium gas was used for ablation initial transport from the laser cell, and this was combined with argon outside the cell as the sample was transported to the ICP-MS. Thermo Elemental PlasmaLab time-resolved analysis (TRA) data acquisition software was used with a total acquisition time of 60 s per analysis, allowing ~30 s for background followed by 25 s for laser ablation. PlasmaLab was used for initial data reduction with post-processing in Excel. The rutile calibration employed BIR-1G, BHVO-2G, and BCR-2G (U.S. Geological Survey [USGS] basalt glass standards) to produce a 4 point (including the origin) calibration curve. The data were normalized to Ti (98% TiO_2) and adjusted accordingly. Instrumental drift was monitored by repeat analysis of BHVO-2G after every 25–30 grains.

The LA-ICP-MS system used at the Central Analytical Facility (CAF), Stellenbosch University (South Africa), consists of an excimer laser system emitting at 193 nm (Resonetics Resolution SE50 utilizing an ATL Atlex laser source) coupled to an Agilent 8800 triple quadrupole ICP-MS. Trace-element data were obtained by single-spot analysis using a 70 µm beam diameter. Ablation was performed using a S155 double-helix ablation cell (Laurin Technic, Canberra, Australia) in helium (325 ml/min) that was mixed in a conical ablation cup into the argon sample gas (950 ml/min) and N_2 (4.1 ml/min) and transferred in Nylon 10 tubing to the mass spectrometer. The isotope used for internal standardization was 49Ti, and National Institute of Standards and Technology (Standard Reference Material) NIST SRM 610 standard reference glass (values from Pearce et al., 1997) was used as external calibration standard. In a typical analytical sequence, one standard was analyzed, followed by 10–15 unknowns, then one standard, and so on. For each analysis, an ablation time of 20 s was applied. Background was measured for 20 s prior to ablation. Data acquisition was performed by peak hopping measuring 1 sample per peak. Reduction of time-resolved data and concentration calculations were subsequently performed off-line using the GLITTER software package. Regular analysis of the BCR-2 standard reference glasses were performed for quality control, and the results are consistently within 2σ of the average concentrations reported by Jochum and Nehring (2006). The detection limit for most of the elements is in the lower ppb to mid ppt range.

Rutile trace-element compositions are sensitive both to host-rock lithology (metamafic and metapelitic rocks) and to metamorphic grade (Meinhold, 2010). Discrimination of rutiles from metamafic and metapelitic provenances was achieved using Cr and Nb contents as described by Meinhold et al. (2008), with metamorphic temperatures estimated on the basis of Zr contents using the formula proposed by Watson et al. (2006).

U-Pb Zircon Age Determination

U-Pb age data were obtained by laser ablation–magnetic sector field–inductively coupled plasma-mass spectrometry (LA-SF-ICP-MS) at the CAF, employing a Thermo Finnigan Element2 mass spectrometer coupled to a New Wave UP213 laser ablation system. All age data presented here were obtained by single-spot analyses with a spot diameter of 30 µm and a crater depth of ~15–20 µm, corresponding to an ablated zircon mass of ~150–200 ng. The methods employed for analysis and data processing are described in detail by Gerdes and Zeh (2006)

and Frei and Gerdes (2009). For quality control, the Plešovice (Sláma et al., 2008) and M127 (Nasdala et al., 2008; Mattinson, 2010) zircon reference materials were analyzed, and the results were consistently in excellent agreement with the published isotope dilution–thermal ionization mass spectrometer (ID-TIMS) ages. Full analytical details and the results for all quality control materials analyzed are reported in Table 1. Plotting of concordia diagrams was performed using Isoplot/Ex 3.0 (Ludwig, 2003), with probability density distribution and histogram diagrams generated by AgeDisplay (Sircombe, 2004).

HEAVY-MINERAL PROVENANCE CHARACTERISTICS

UK Well 164/25-1ST

The heavy-mineral assemblages in 164/25-1ST are dominated by garnet and apatite, which form up to 86% and 33% of individual samples, respectively. In the shallowest cuttings samples, clinopyroxene is abundant (up to 80%), and is found together with minor epidote and titanite. These minerals are considered to represent contamination from the overlying Paleogene basaltic succession.

Provenance-sensitive, heavy-mineral parameters (Fig. 4) indicate the succession is characterized by very high GZi (93–99), very high ATi (89–100), and very low ARi (0–5). RuZi shows a downhole increase, with values of 22–40 in the upper part (3420–3629 m inclusive) and 40–61 in the lower part (3674–4040 m inclusive). Other parameters (MZi and CZi) remain consistently low throughout.

The extremely high GZi and ATi, together with the very low ARi, suggest the sandstones are of first-cycle origin, since recycled material is normally characterized by lower apatite and garnet due to the relative instability of these minerals during weathering, and prolonged sediment transport is likely to result in increased ARi. The upward decrease in RuZi indicates a change from rutile-rich to rutile-poor (relative to zircon) sources with time.

Garnet assemblages (Fig. 5) are dominated by high-Mg, low-Ca types (Type A) throughout. Garnets in the shallowest sample (3520 m) have generally lower Mg contents than in the rest of the succession, where Type Ai garnets (those with X_{Mg}>30%) are dominant. This change in garnet composition coincides with the upward decrease in RuZi noted above and suggests a change in source area characteristics.

Rutile compositions (Fig. 6) also indicate a change in provenance characteristics through the succession. The two deeper samples have high proportions of granulite-facies rutiles (crystallization temperatures >750 °C), whereas the shallowest sample (3520 m) has a much higher proportion of amphibolite-facies grains. In addition, there is a change in relative proportion of rutiles of metamafic and metapelitic parentage in the interval dominated by high-grade metamorphic detritus, with metamafic grains being more prevalent in the younger sample.

Zircon age determinations were made on the same three samples as for rutile geochemistry (Fig. 7). The three samples share certain common features, with all having a major peak at ca. 1900 Ma together with a wider-ranging Archean group mainly falling in the 2600–2900 Ma age range. However, the shallowest sample is distinctive in showing a major peak at ca. 2100 Ma, which is poorly represented in the deeper section. Furthermore, the two deeper samples contain a group of Permian zircons (ca. 258–299 Ma) not represented in the upper sample. The abundance of this group decreases with time, with the deepest sample containing 12 grains of this age (22% of the zircons with <10% discordance), whereas the overlying sample has only six grains (8% of the zircons with <10% discordance). The presence of this group indicates a maximum depositional age of mid-Permian for the succession, defined by the presence of three zircons at 266 ± 5 Ma, 267 ± 5 Ma, and 267 ± 5 Ma. The youngest zircon (258 ± 6 Ma) has more doubtful significance owing to its lower concordance (93.4% compared with 96.8%–99.5%).

Strathmore Field (UK Blocks 204/30 and 205/26, West of Shetland)

Heavy-mineral, garnet geochemistry, and U-Pb zircon age data from Triassic sandstones of the Strathmore Field published by Morton et al. (2007) have been supplemented by rutile geochemical data and by an additional zircon age determination acquired during the current study. The succession in the Strathmore Field includes the Otter Bank Formation, of probable Scythian age, and the Foula Formation, of probable Ladinian–Carnian age (Swiecicki et al., 1995). There is a distinct change in heavy-mineral characteristics between these two units (Fig. 4). The Otter Bank Formation is characterized by relatively low RuZi, high GZi, and ATi that is moderate in the lower part and high approaching the top. The Foula Formation has extremely high GZi and ATi, with RuZi generally high but with lower values in at least two zones. These variations have been used for field-scale correlation purposes (Morton et al., 2007).

Evidence for a major change in provenance between the Otter Bank and Foula formations is also given by garnet and rutile compositions (Figs. 5 and 6) and zircon U-Pb data (Fig. 7). The Otter Bank Formation is characterized by low-Mg, variable-Ca garnet populations that correspond to Type B (Fig. 5), with minor representation of Types A and C, whereas the Foula Formation has assemblages dominated by the Type Ai component.

Rutile assemblages in the Otter Bank Formation from 205/26a-4 are diverse but dominated by amphibolite-facies grains, whereas the Foula Formation is characterized by abundant granulite-facies rutile. Rutile compositions within the Foula Formation from the same well show more variation than the associated garnets, which are consistently rich in the Type Ai component (Fig. 5). The variability in rutile composition is manifested by fluctuations in the relative proportion of grains of metamafic and metapelitic parentage (Fig. 6), as well as variations in the crystallization temperature distribution. Most notably, the deepest Foula Formation sample has a high proportion of upper-amphibolite rutiles than the overlying samples, possibly suggesting progressive unroofing of high-grade lithologies. It is also notable that the shallowest sample in 205/26a-4 shows the reappearance of lower-grade (amphibolite-facies) detritus associated with a slight fall in RuZi (Fig. 4). This may be a precursor to the larger-scale cyclicity in RuZi seen higher in the Foula Formation in 204/30a-2 (Fig. 4).

TABLE 1. LA-SF-ICP-MS U-Th-Pb DATING METHODOLOGY, CAF, STELLENBOSCH UNIVERSITY

Laboratory and sample preparation	
Laboratory name	Central Analytical Facility, Stellenbosch University
Sample type and mineral	Detrital zircons
Sample preparation	Conventional mineral separation, 1 inch resin mount, 1 µm polish to finish
Imaging	Cathodoluminescence, Zeiss Merlin, 10 nA, 15 mm working distance
Laser ablation system	
Make, model, and type	Resonetics Resolution S155, ArF Excimer
Ablation cell and volume	Laurin Technology S155 double Helix large volume cell
Laser wavelength	193 nm
Pulse width	20 ns
Fluence	~2 J/cm^{-2}
Repetition rate	5.5 Hz
Spot size	30 µm
Sampling mode and pattern	30 µm single-spot analyses
Carrier gas	100% He, Ar make-up gas combined using a T-connector close to double Helix sampling funnel
Pre-ablation laser warm-up (background collection)	Three cleaning shots followed by 20 seconds background collection
Ablation duration	15 seconds
Wash-out delay	15 seconds
Cell carrier gas flow	300 ml/min He and 0.06 ml/min N_2
ICP-MS Instrument	
Make, model, and type	Thermo Finnigan Element2 single collector HR-SF-ICP-MS
Sample introduction	Via conventional tubing
Radio frequency power	1350 W
Make-up gas flow	1.0 l/min Ar
Detection system	Single-collector secondary electron multiplier
Masses measured	202, 204, 206, 207, 208, 232, 233, 235, 238
Integration time per peak	4 ms
Total integration time per reading	1 sec *(represents the time resolution of the data)*
Sensitivity	30,000 cps/ppm Pb
Dead time	6 ns
Data Processing	
Gas blank	20 second on-peak
Calibration strategy	GJ-1 used as primary reference material; M127 and 91500 used as secondary reference material (Quality Control).
Reference material info	M127 (Nasdala et al., 2008; Mattinson, 2010), 91500 (Wiedenbeck et al., 1995), GJ-1 (Jackson et al., 2004).
Data processing package used Correction for LIEF	In-house spreadsheet data processing using intercept method for LIEF correction.
Mass discrimination	Standard-sample bracketing with $^{207}Pb/^{206}Pb$ and $^{206}Pb/^{238}U$ normalized to reference material GJ-1.
Common-Pb correction, composition, and uncertainty	^{204}Pb method, Stacey and Kramers (1975) composition at the projected age of the mineral, 5% uncertainty assigned.
Uncertainty level and propagation	Ages are quoted at 2 sigma absolute; propagation is by quadratic addition. Reproducibility and age uncertainty of reference material and common-Pb composition uncertainty are propagated.
Quality control and validation	91500: Concordia age = 1072.9 ± 6.2 (2σ , n = 10, MSWD = 0.28) M127: Weighted concordia age = 528.8 ± 2.1 (2σ, n = 15, MSWD = 0.32)

Note: For detailed method description, see Frei and Gerdes (2009). Abbreviations: CAF—Central Analytical Facility; HR-SF—high-resolution sector field; LA-SF-ICP-MS—laser ablation-magnetic sector field inductively coupled plasma-mass spectrometry; LIEF—laser induced elemental fractionation; MSWD—mean square of weighted deviates.

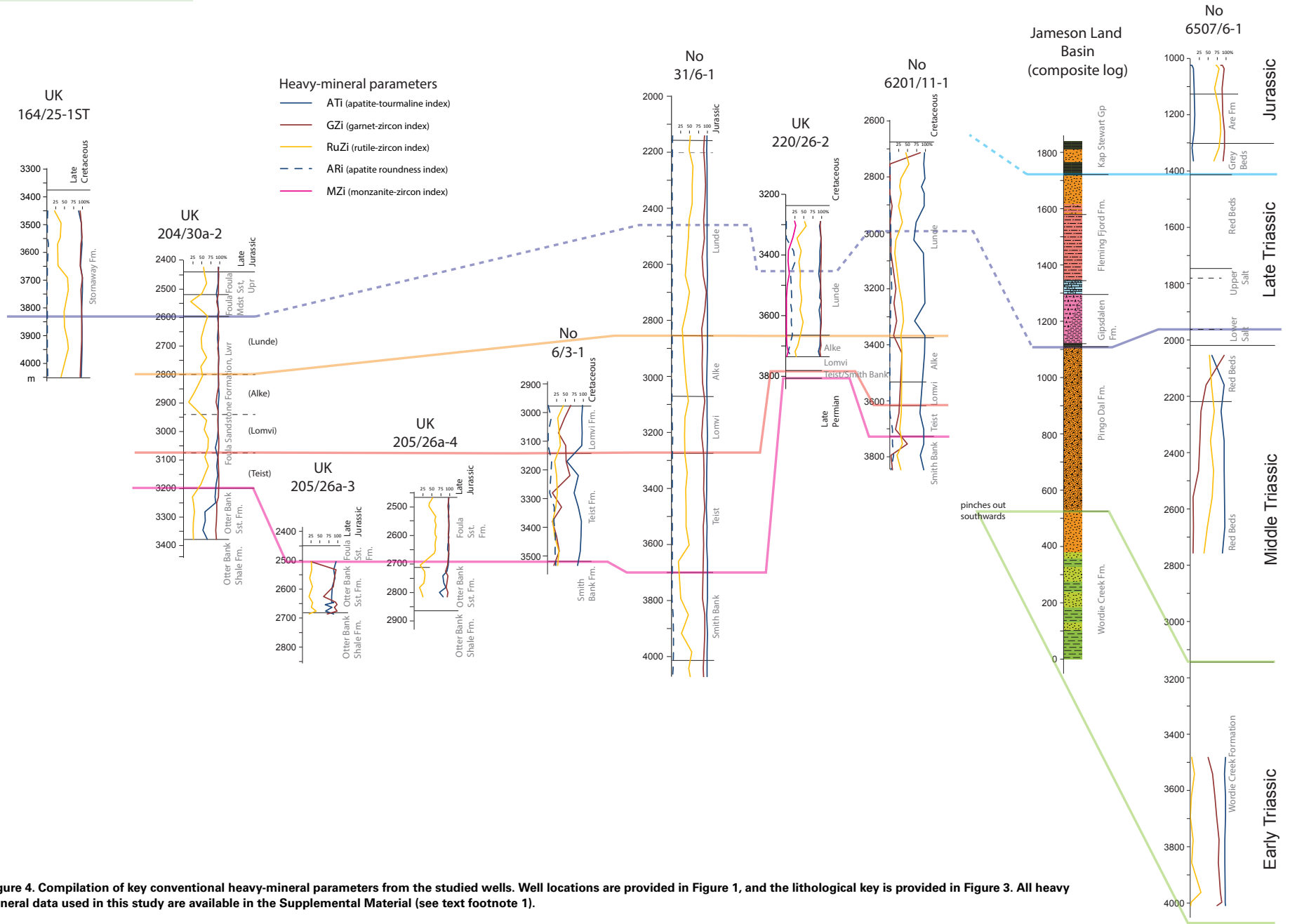

Figure 4. Compilation of key conventional heavy-mineral parameters from the studied wells. Well locations are provided in Figure 1, and the lithological key is provided in Figure 3. All heavy mineral data used in this study are available in the Supplemental Material (see text footnote 1).

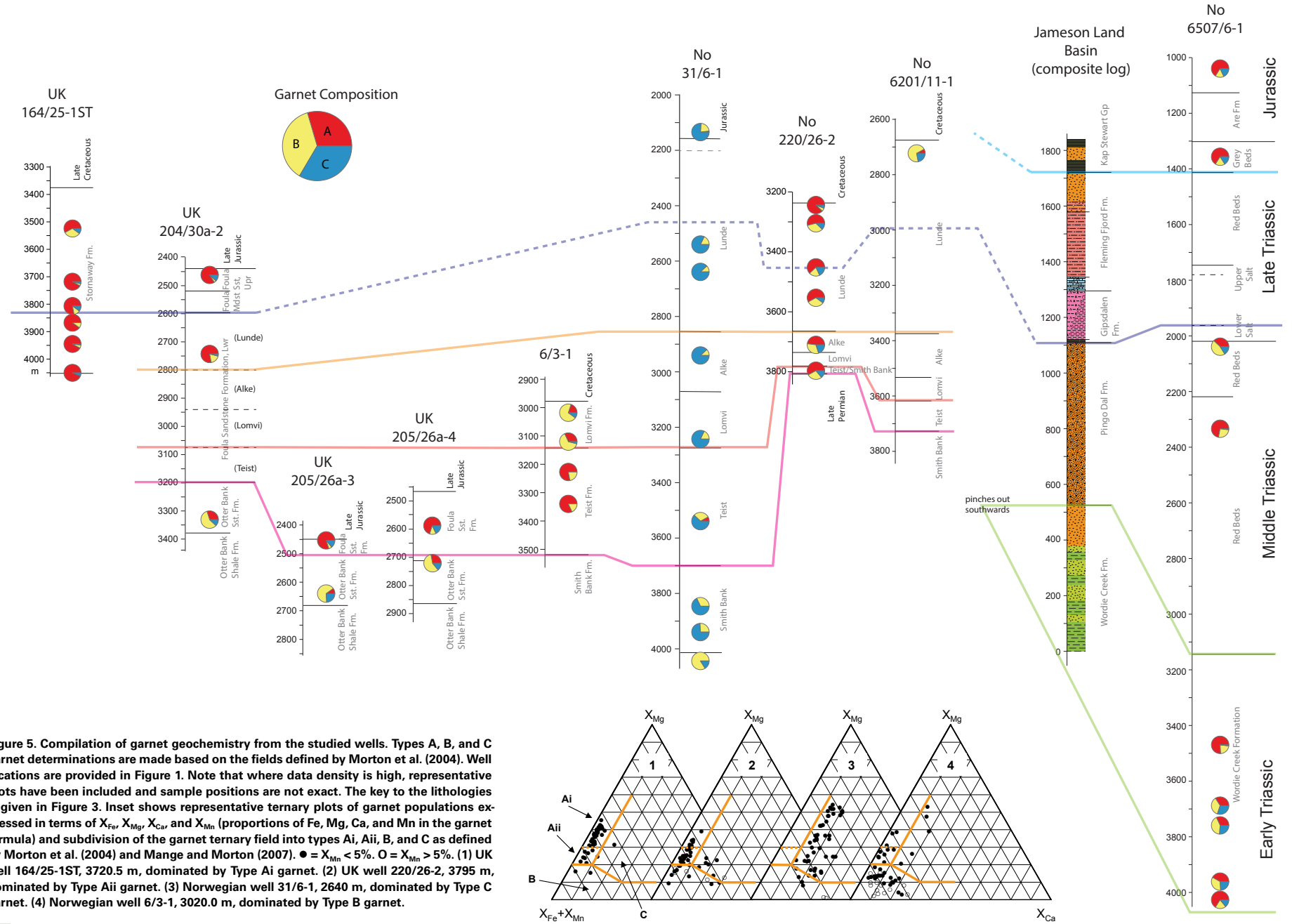

Figure 5. Compilation of garnet geochemistry from the studied wells. Types A, B, and C garnet determinations are made based on the fields defined by Morton et al. (2004). Well locations are provided in Figure 1. Note that where data density is high, representative plots have been included and sample positions are not exact. The key to the lithologies is given in Figure 3. Inset shows representative ternary plots of garnet populations expressed in terms of X_{Fe}, X_{Mg}, X_{Ca}, and X_{Mn} (proportions of Fe, Mg, Ca, and Mn in the garnet formula) and subdivision of the garnet ternary field into types Ai, Aii, B, and C as defined by Morton et al. (2004) and Mange and Morton (2007). ● = X_{Mn} < 5%. O = X_{Mn} > 5%. (1) UK well 164/25-1ST, 3720.5 m, dominated by Type Ai garnet. (2) UK well 220/26-2, 3795 m, dominated by Type Aii garnet. (3) Norwegian well 31/6-1, 2640 m, dominated by Type C garnet. (4) Norwegian well 6/3-1, 3020.0 m, dominated by Type B garnet.

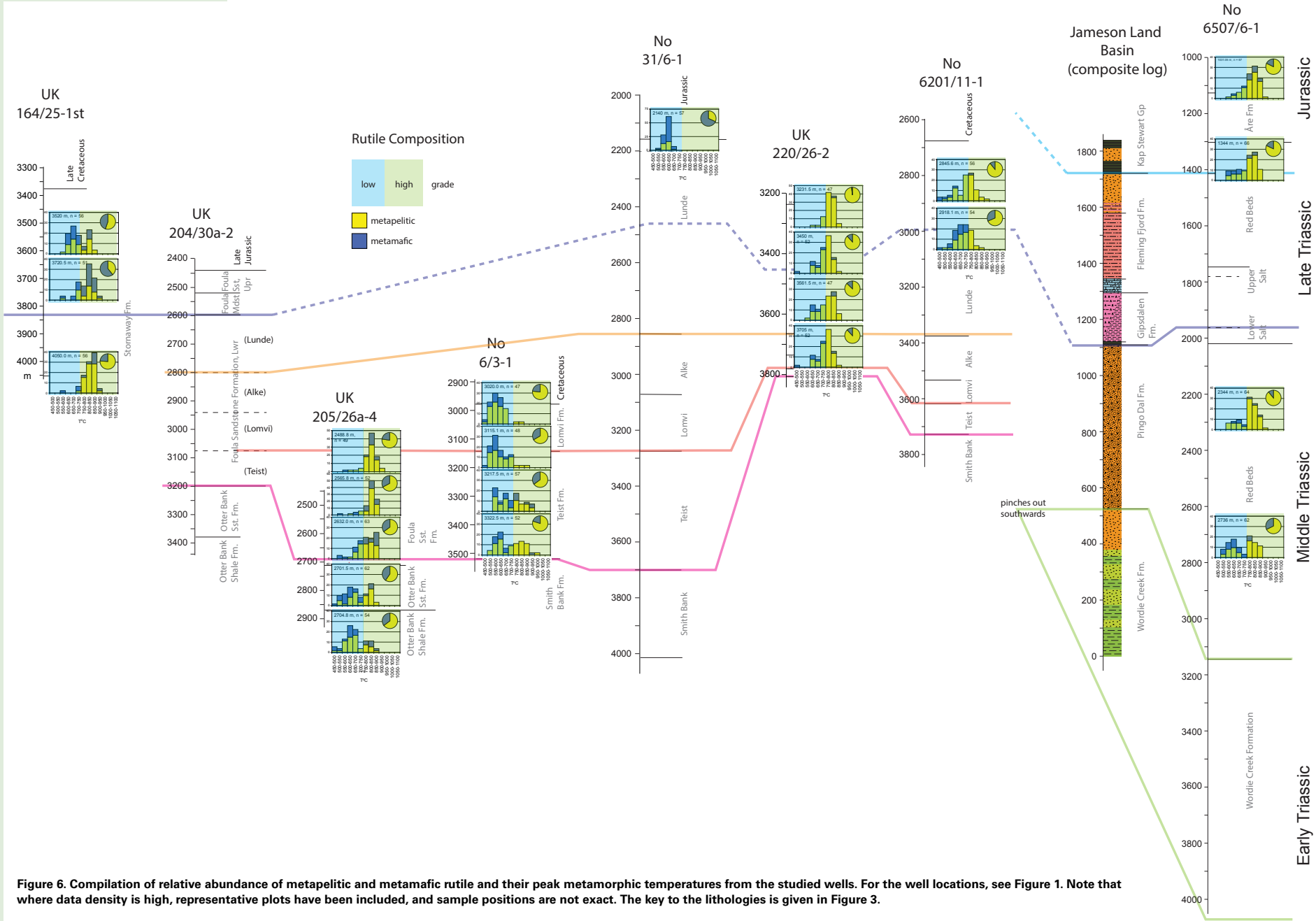

Figure 6. Compilation of relative abundance of metapelitic and metamafic rutile and their peak metamorphic temperatures from the studied wells. For the well locations, see Figure 1. Note that where data density is high, representative plots have been included, and sample positions are not exact. The key to the lithologies is given in Figure 3.

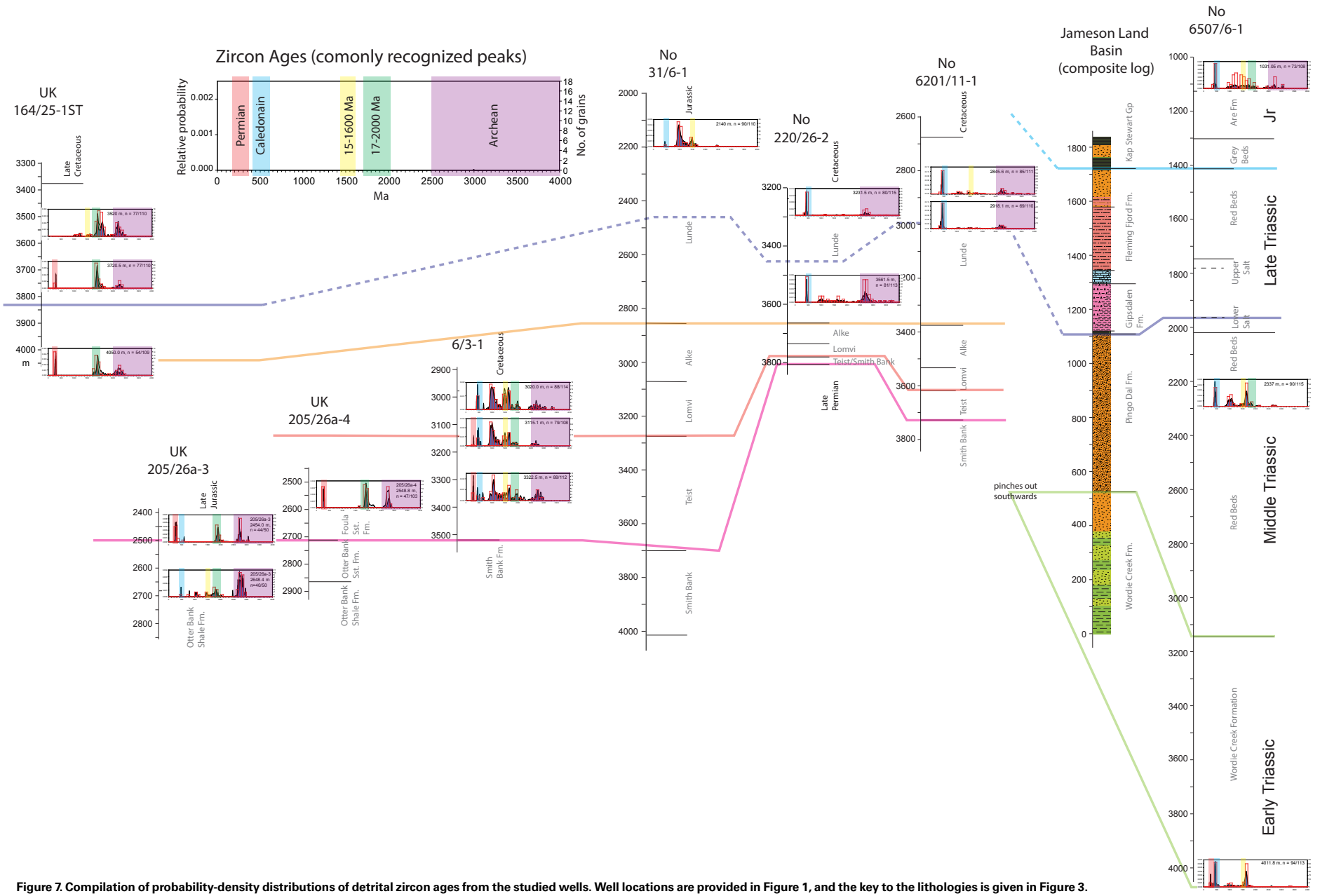

Figure 7. Compilation of probability-density distributions of detrital zircon ages from the studied wells. Well locations are provided in Figure 1, and the key to the lithologies is given in Figure 3.

Zircon age data confirm a marked difference in provenance between the Otter Bank and Foula formations (Fig. 7). The zircon spectrum in the Otter Bank sample has a large Archean group between 2600 Ma and 3000 Ma, together with a range of mid-Proterozoic grains mostly in the 1000–2000 Ma range, and a very small early Paleozoic component. The Foula Formation samples also have large Archean components but differ in having a single, well-defined Paleoproterozoic peak at ca. 1900 Ma, together with a group of Permian zircons (255–301 Ma). The Permian group forms 25% of the near-concordant zircon population in the basal Foula Formation sample from 205/26a-3 and 23% of a sample some 150 m above the base in 205/26a-4 (Fig. 7).

UK Well 220/26-2

The Triassic sandstones in 220/26-2 are comparable to those in 164/25-1ST and in the Foula Formation of the Strathmore area, in that garnet is the dominant heavy-mineral phase throughout, forming 61%–91% of the assemblages. Epidote is also common, forming up to 22% of the assemblages, but only in the lower part of the analyzed interval (3450–3975 m inclusive).

Provenance-sensitive, heavy-mineral parameters (Fig. 4) show that the entire succession is characterized by very high ATi and GZi (94–100 and 96–99, respectively). RuZi shows an overall upward increase, with comparatively low values at the base, moderate through the majority of the section, and relatively high at the top. ARi also shows a significant upward change, with the majority of the succession having comparatively high values (up to 25), but low in the topmost three samples (3231–3300 m inclusive). These three samples are also distinctive in having markedly higher MZi values (19–26, compared with 0–8 in the underlying interval).

The presence of epidote at depths exceeding 3400 m is anomalous, since this mineral is unstable during burial diagenesis. Its presence suggests that porosity and permeability are low, thereby inhibiting pore-water movement and decreasing the potential for dissolution of unstable minerals. The presence of epidote cannot be attributed to contamination of cuttings samples since it also occurs in a core sample in the same interval. The upward disappearance of epidote suggests that reservoir quality improves higher in the succession.

The very high ATi and GZi suggest much of the detritus is first-cycle, as does the presence of epidote in the deeper part of the well. However, it is evident from the coincidental changes in MZi and ARi toward the top of the succession that there was a change in provenance and transport history between 3355 m and 3300 m. This change is coincident with a shift in garnet compositions (Fig. 5), rutile compositions (Fig. 6), and zircon ages (Fig. 7).

Garnet assemblages (Fig. 5) are consistently dominated by the Type A component, but in the lower part of the succession, Mg contents are generally lower than at the top. Furthermore, the assemblages in the lower part include higher proportions of Type C (high-Ca, high-Mg) grains. Rutile populations are likewise dominated by granulite-facies grains throughout, but the proportion increases toward the top of the succession (54%–57% in the lower three samples, 83% at the top of the interval). This is accompanied by an increase in proportion of metapelitic grains at the expense of metamafic varieties (87%–88%, rising to 98%).

Zircons were analyzed from two samples to evaluate the nature of the change in mineralogy and mineral chemistry. Both samples are distinctive in having a large early Paleozoic peak and an Archean group, but the lower sample contains a range of mid-Proterozoic zircons that are poorly represented in the upper sample (Fig. 7). Archean (and earliest Paleoproterozoic) zircons form 57% and 40% of the assemblages in the lower and upper samples, respectively. Most of these ages lie between ca. 2600 Ma and ca. 2900 Ma, but a substantial number are older, the oldest being ca. 3700 Ma. The early Paleozoic group comprises 20% in the lower sample and 54% in the upper, in both cases forming a peak at ca. 430 Ma (Fig. 7). Mid-Proterozoic zircons, which form 23% of the population in the lower sample compared with only 6% in the upper, are wide ranging (900–1880 Ma) and polymodal, with notable peaks in the 1000–1200 Ma, 1600–1700 Ma, and 1800–1900 Ma intervals.

Norwegian Well 6201/11-1

Well 6201/11-1 is located in the southern part of the Møre Basin, and is reasonably close to UK well 220/26-2 (Fig. 1). The succession is attributed to the Hegre Group, with the Lunde, Alke, Lomvi, and Teist formations all recognized (Fig. 3). Data quality from this well is relatively poor because most of the samples were small-volume ditch cuttings and were heavily contaminated by the mud-weighting additive barite. However, reasonably good data were acquired from the core in the topmost part of the analyzed interval. In addition, it is evident from the samples that heavy-mineral dissolution has been pervasive. Garnet is scarce in most cases, and where present, shows signs of extreme corrosion. It is found in abundance in just one sample, the shallowest core sample, and its presence indicates it is likely to have been abundant throughout prior to burial diagenetic modification.

The downhole plot of provenance-sensitive, heavy-mineral parameters (Fig. 4) shows that ATi is extremely high throughout, apart from sporadic cuttings from samples with suspect data owing to comparatively low grain counts. GZi is generally low, but this is due to garnet depletion during burial diagenesis. Only one sample, at the very top of the cored section, contains abundant garnet (high GZi). RuZi is moderate throughout, but is higher in the top two core samples: this increase may mark a change in provenance. ARi is low in most samples, but values are somewhat higher near the base (Teist Formation).

As with the other wells in the study, the high ATi values and originally high GZi values indicate a likely first-cycle origin for the Triassic succession in 6201/11-1. There is a hint of a change in provenance near the top of the well, on the basis of the increase in RuZi, and the higher ARi values in the Teist Formation suggest more prolonged transport history at this time.

Acquisition of further constraints on provenance of the succession is limited by the general scarcity of garnet and by the poor recovery of heavy minerals

from the cuttings samples. Garnet geochemistry was undertaken on the only garnet-rich sample, with rutile and zircon data acquired from two core samples lower down in the succession (Figs. 6 and 7).

The garnet assemblage in the sample from 2729.45 m (Fig. 5) is dominated by low-Mg, variable-Ca grains (Type B), with minor representation of Type C and scarce Type A. The rutile assemblages from deeper in the core (2845.6 m and 2918.1 m) are broadly similar to one another, both having wide-ranging crystallization temperatures including relatively high proportions of granulite-facies grains (Fig. 6). The deeper sample has fewer granulite-facies grains (24%) and high proportions of metamafic grains (31%) compared with the shallower sample (43% and 11%, respectively).

Both analyzed zircon assemblages are dominated by the early Paleozoic group, which forms 49%–77% of the near-concordant populations and peaks in the 430–440 Ma range (Fig. 7). The remainder of the zircon spectra contain a wide-ranging mid-Proterozoic group (ca. 870–2030 Ma), which forms 6%–24% of the populations, and an Archean group that mainly lies in the ca. 2600–2900 Ma range but extends back to 3760 Ma, which forms 17%–27% of the populations.

There are no additional constraints on the provenance of the underlying uncored interval, although the general uniformity of the heavy-mineral assemblages suggests little change. Ideally, this section should be revisited using larger-volume unwashed ditch cuttings if they were available. Furthermore, rutile and zircon data should be acquired from the sample with garnet geochemistry, since the garnet data from this sample suggest a lower-grade metamorphic source compared with the underlying interval with rutile geochemical data. It was not possible to undertake rutile or zircon analyses from the garnet-rich sample owing to the small size of the available sample.

Norwegian Well 31/6-1

Well 31/6-1, located in the northern North Sea adjacent to the Norwegian landmass (Fig. 1), encountered a thick Triassic section. Most of the samples analyzed from this well are attributed to the Hegre Group, but the topmost sample is from the Statfjord Group (Rhaetian–Sinemurian), and the lowermost three belong to an undefined group overlying basement (Fig. 3).

With the exception of the Statfjord Group sample, the heavy-mineral characteristics of the analyzed interval are remarkably uniform. Epidote is dominant throughout, forming up to 80% of the assemblages, with titanite, garnet, and apatite forming the majority of the rest. Provenance-sensitive, heavy-mineral parameters are likewise uniform (Fig. 4), with extremely high ATi (95–100), high GZi (78–96), and low-moderate RuZi (18–57). RuZi shows an upward increase at ~2700 m. The increased scatter in RuZi toward the base of the analyzed interval is likely to be a function of comparatively low grain counts rather than of genuine fluctuations. Apatite roundness is also extremely low throughout, although values are slightly higher near the base (3840–3987 m).

These heavy-mineral characteristics suggest first-cycle derivation. The abundance of epidote throughout suggests that porosity and permeability are low, inhibiting dissolution of this unstable mineral (as discussed in the section on well 220/26-2).

The single Statfjord Group sample is markedly different, with considerably lower ATi and GZi, and an absence of epidote. It is difficult to determine on the heavy-mineral data alone whether this change is a function of changing provenance or to the response of the mineralogy to the changing climate associated with the Triassic–Jurassic transition.

Further constraints on provenance of the Hegre Group and the changes observed at the base of the Statfjord Group have been acquired using garnet geochemical analysis (Fig. 5). The data show uniformity of provenance throughout the Hegre Group and into the Statfjord Group, with virtually all samples being dominated by high-Ca, high-Mg grains that conform to Type C of Mange and Morton (2007). The only exception is the sample at the very base of the analyzed interval (4067 m), in which Type C garnets are subordinate to a group of high-Mn, high-Ca grains with very low Mg contents (Type B). This sample is from the basement underlying the Triassic interval, and indicates that the immediately subjacent basement has a different metamorphic character to the source of the overlying sediment.

Since garnet data show uniformity of provenance throughout, rutile and zircon analyses were carried out on just one sample. The sample chosen was the one from the Statfjord Group, since this is much richer in zircon and rutile compared with the apatite-epidote-garnet suites associated with the Hegre Group. The rutile population is distinctive, being dominated by metamafic varieties (68% of the assemblage) with formation temperatures that equate to lower amphibolite and/or eclogite facies (Fig. 6). The zircon spectrum is dominated by a group peaking between ca. 890–1130 Ma, which forms 68% of the near-concordant zircon population. The remainder of the population is virtually exclusively Mesoproterozoic, with a conspicuous peak in the 1400–1500 Ma range. Early Paleozoic and Archean zircons are very scarce.

Norwegian Well 6/3-1

The heavy-mineral assemblages in the Skagerrak Formation (Triassic) of 6/3-1, located toward the southern end of the Viking Graben, are dominated by apatite (15%–70%), zircon (4%–32%), and garnet (4%–35%). Most garnet grains show corrosion textures, and the severity of the etching increases with depth. Hence, the relatively low garnet contents in this well are attributed to burial-related garnet dissolution.

The downhole plot of provenance-sensitive parameters from 6/3-1 (Fig. 4) shows that ATi values are high through most of the succession. Values in core are very high (96–98) and are also high (up to 95) in cuttings deeper in the well. However, they are low immediately below the cored interval and then show a gradual rise with increasing depth. These low values may be anomalous, due to downhole contamination following re-entering of the well after the core was taken.

GZi values are comparatively low and show an overall decrease downhole. Given the evidence for increasing garnet dissolution with depth, this trend is interpreted as the result of progressive burial-related loss of garnet. Therefore, GZi values in this well are not considered to be truly representative of the source area characteristics, and are likely to have been higher prior to burial. RuZi shows a subtle upward increase but the change takes place at the switch from cuttings to core material and may therefore not be a reliable indicator of a change in provenance. The only reliable change in mineral characteristics in 6/3-1 is the upward decrease in apatite roundness, which is high in the lower part of the well (below 3300 m) and low higher up. This change takes place within the cuttings data set and can therefore be considered genuine.

Additional provenance constraints were acquired by undertaking garnet and rutile geochemistry on four samples, with zircon dating on three of these four samples. The garnet and rutile data indicate that there was a change in provenance character within the succession. The samples from the upper part of the succession (3020.0 m and 3115.1 m) have garnet assemblages rich in the Type B component, with subordinate Types A and C, whereas those from 3217.5 m and 3322.5 m are rich in Type A, with the majority of these corresponding to Type Ai (Fig. 5). The generally low Ca content of the garnets in 6/3-1 may be partly due to garnet dissolution, which is evident from the garnet surface textures. High-Ca garnets are less stable than Ca-poor types (Morton and Hallsworth, 2007), and hence progressive garnet dissolution tends to result in increased abundances of low-Ca garnets. However, the change observed in 6/3-1 cannot be ascribed to garnet dissolution since it is expressed by differences within the low-Ca part of the garnet populations. Furthermore, the change from Type Ai–dominated to Type B–dominated garnet populations coincides with a change from high-grade to lower-grade rutile assemblages (Fig. 6). Granulite-facies rutiles comprise 40% of the assemblages in the deepest samples (3217.5 m and 3322.5 m) but only 4%–6% in the upper part of the section.

The two samples from the upper part of the Triassic have closely comparable zircon age populations (Fig. 7), both being dominated by wide-ranging mid-Proterozoic zircons with distinct peaks at ca. 1000 Ma, ca. 1500 Ma, and ca. 1650 Ma, together with subordinate early Paleozoic groups (ca. 400–480 Ma), and minor Archean representation. The deeper sample is also dominated by mid-Proterozoic zircons with a subordinate early Paleozoic group, but the mid-Proterozoic peaks are in slightly different positions, and there is a more distinct representation of Paleoproterozoic grains between ca. 1900–2100 Ma. In addition, the Archean is better represented, and there is a distinct group of five Permian zircons (263–287 Ma) that have virtually no counterpart in the overlying interval.

Nordland Ridge (Norwegian Wells 6507/6-1 and 6608/8-1)

Well 6507/6-1 encountered a thick Triassic section, with the Rhaetian–Pliensbachian Åre Formation overlying sandstones and mudstones that are believed to have an Early to Late Triassic age. These have not been given formal lithostratigraphic names ("Grey Beds" and "Red Beds"), although the deepest unit is interpreted as equivalent to the Wordie Creek Formation (Fig. 3).

The heavy-mineral stratigraphic profile (Fig. 4) shows that the Åre Formation is characterized by low ATi in association with high GZi and high RuZi, closely comparable to features shown by the Åre Formation in the Heidrun Field, Norwegian block 6507/8-1 (Morton et al., 2009a). Garnets from this interval (Fig. 5) are dominated by high-Mg, low-Ca types (Type A), as also found in the Åre Formation from Heidrun (Morton et al., 2009a). The associated rutile populations (Fig. 6) are rich in granulite-facies grains, mainly of metapelitic parentage. The zircon spectrum (Fig. 7) has a well-defined early Paleozoic peak (ca. 370–500 Ma) consisting of 15 of the 73 near-concordant grains, a wide-ranging mid-Proterozoic group (ca. 920–2020 Ma) comprising 48 zircons, and a small Archean group of ten zircons between ca. 2400–3100 Ma. The mid-Proterozoic zircons form a broad and somewhat diffuse group without well-defined peaks, but the early Paleozoic group shows a clear peak in the 430–440 Ma bracket. A closely comparable zircon age distribution is present in the Åre Formation of the Heidrun Field (figure 6 in Morton et al., 2009a).

The sandstones sampled between 2064 m and 2766 m have markedly different mineralogy to the Åre Formation, with very high ATi, generally low GZi (with a downhole-decreasing trend) and high RuZi. The downhole-decreasing GZi pattern is probably attributable to progressive garnet dissolution with increasing burial depth, and values were likely to have been higher at the time of deposition. Garnet compositions (Fig. 5) are comparable to those in the Åre Formation, with Type A dominant, and a similar source is considered possible. Rutile compositions are also similar to those in the Åre Formation, although the deeper of the two analyzed samples has a more diverse rutile population, containing granulite-facies and amphibolite-facies grains in approximately equal proportions (Fig. 6). The contrast in ATi between the Åre Formation and the underlying sandstones is interpreted as the result of apatite depletion through weathering related to the more humid climate during the Rhaetian–Pliensbachian. The zircon spectrum (Fig. 7) has early Paleozoic, mid-Proterozoic, and Archean representation, but differs from the Åre Formation in that the Archean group is poorly represented, and the mid-Proterozoic group is characterized by two well-defined peaks (ca. 1000–1200 Ma and ca. 1600–1700 Ma) rather than the broader and more diffuse grouping shown by the shallower sample.

The lowest sand package (sampled at 3483–4011.8 m inclusive) is also characterized by high ATi, but differs in having higher GZi and much lower RuZi. The markedly lower RuZi implies derivation from a different source region, scarce in rutile-bearing lithologies. Garnets in the lowest sand package are diverse and include both Type B and Type C in addition to variable numbers of Type A grains. The zircon spectrum has two clearly defined peaks, one in the early Paleozoic and one in the late Paleoproterozoic (1600–1700 Ma). These peaks are also evident in the sample from the middle package, but the ca. 1000–1200 Ma peak is much more subdued and the Archean is almost completely absent. The sample is also distinctive in containing five Permian–Triassic zircon grains dated between 245 Ma and 262 Ma.

In addition to the data acquired from 6507/6-1, two samples were analyzed from a core in the "Red Beds" from 6608/8-1. These samples have high ATi and high RuZi, similar to the middle sand package in 6507/6-1, although they differ in having higher GZi. The garnet population is similar to that seen in the middle package in 6507/6-1, in that it contains large numbers of Type A garnet (Fig. 5), but it differs in that it has a larger proportion of high-Ca garnet. The differences in GZi and garnet compositions between the two wells are interpreted as the result of more advanced garnet dissolution in 6507/6-1, since high-Ca garnet is less stable than low-Ca garnet during burial diagenesis.

The rutile population in 6608/8-1 is clearly bimodal, with a group of granulite-facies rutiles with largely metapelitic compositions and another lower-grade group with both metapelitic and metamafic parentage. This population is very similar to that seen in the sample at 2736 m in 6507/6-1 (Fig. 6), suggesting that the analyzed interval in 6608/8-1 correlates with the lower part of the middle package in 6507/6-1.

The zircon spectrum from 6608/8-1 is also comparable with that in the middle package of 6507/6-1 (Fig. 7), although it displays a peak in the 1400–1500 Ma interval, which is poorly represented in 6507/6-1.

DISCUSSION

The heavy-mineral evidence from these widely spaced locations in the NE Atlantic reveals that there are major variations in provenance, both regionally and stratigraphically. On the basis of data collected to date, five distinct provenance domains can be defined: the northern Rockall Trough and southern Faroe-Shetland Basin; the northern margin of the Shetland Platform and southern Møre Basin; the northeastern part of the North Sea; the Viking Graben; and the Nordland Ridge (Fig. 8).

Northern Rockall Trough and Southern Faroe-Shetland Basin

The provenance characteristics of the succession in well 164/25-1ST closely match those seen in the Foula Formation of the Strathmore area, especially in the lower part of the Rockall Trough well, and a common provenance is clearly indicated (Figs. 4–7). The key features of these sandstones are (1) abundant garnet with dominantly Type A compositions, (2) high rutile:zircon indices with rutile of mainly granulite-facies origin, and (3) zircon age spectra with peaks in the Permian, Paleoproterozoic (ca. 1900 Ma), and Archean (ca. 2700 Ma).

On the basis of these data, Morton et al. (2007) proposed derivation from the Nagssugtoqidian belt of southern East Greenland (Fig. 8), which has a suitable geological history comprising Archean crust reworked by metamorphism ca. 1800–1900 Ma (Kalsbeek et al., 1984; Kalsbeek et al., 1993; van Gool et al., 2002) and also provides garnet assemblages rich in the Type A component (Sørensen and Kalvig, 2002; Thrane and Keulen, 2015). Detrital zircons in stream sediments and tills derived from this area have age spectra that match those in the northern Rockall Trough and Strathmore areas (Thrane and Keulen, 2015). Although there are regions of Lewisian crust onshore Scotland that have some features in common with the Foula Formation (Tyrrell et al., 2009), these have very limited regional extent and would not be capable of supplying large amounts of sediment with such distinct character over the relatively wide area implied by the well data. Furthermore, sediment fed from the Lewisian has markedly different features to that associated with the Foula Formation, both in terms of garnet composition (Morton et al., 2004) and zircon ages (Morton et al., 2012). It is possible that the sediment was derived from an alternative source in a more proximal location (Morton et al., 2007), since there is a series of basement highs in the NE Atlantic between the British Isles and East Greenland. The largest of these, the Rockall High, can be ruled out on the basis of zircon age data that indicate this region comprises crust formed ca. 1750–1800 Ma (Daly et al., 1995; Scanlon and Daly, 2001; Morton et al., 2009b; Morton et al., 2014). However, George Bligh High, located farther north, may be a more suitable candidate, since zircons in sediment shed from the George Bligh High include both Archean (2760–2930 Ma) and Paleoproterozoic (1760–1930 Ma) ages (Morton et al., 2014).

There is evidence for stratigraphic evolution in provenance in both 164/25-1ST and the Strathmore area (Figs. 4–7). In the northern Rockall Trough, the detritus becomes somewhat lower grade, and there is a coincident influx of zircons dated ca. 2100 Ma. This is a relatively unusual age group in the NE Atlantic but has been recorded from gneisses in the Ammassilik region of southern East Greenland (Kalsbeek et al., 1993), which provides further support for supply from the Nagssugtoqidian belt of southern East Greenland (Fig. 8). In Strathmore well 205/26a-4, rutile data indicate an increase in supply from a lower-grade metamafic terrain at the top of the Foula Formation, but at present there are no zircon data to indicate if this is accompanied by a change in source area U-Pb age spectra. The change in provenance character may coincide with the boundary between the "lower" and "upper" Foula Formation as defined by Swiecicki et al. (1995), but this requires further evaluation, concentrating on well 204/30a-2, which is believed to penetrate both the lower and upper Foula Formation (Swiecicki et al., 1995, their figure 6).

The other distinctive feature of the Foula Formation and similar sandstones in 164/25-1ST is the presence of the enigmatic Permian zircon group (Fig. 6). The origin of these zircons is discussed further below.

In the Strathmore area, the older part of the Triassic (Otter Bank Formation) has a different provenance, interpreted by Morton et al. (2007) to be recycled Old Red Sandstone with similar characteristics to the Clair Group in the Clair Field (in particular, the Upper Clair Group). Zircon age data from the Clair Group succession provide further support for this suggestion, since the Upper Clair Group zircon population is rich in Archean grains of comparable age to those in the Otter Bank Formation and is similarly comparatively scarce in Early Paleozoic grains (Schmidt et al., 2012). The Otter Bank Formation, however, has a larger mid-Proterozoic zircon component than the Upper Clair Group, likely to indicate that some Lower Clair Group detritus was also recycled. There is no evidence for similar sourcing in the lower part of the analyzed succession in the northern Rockall Trough.

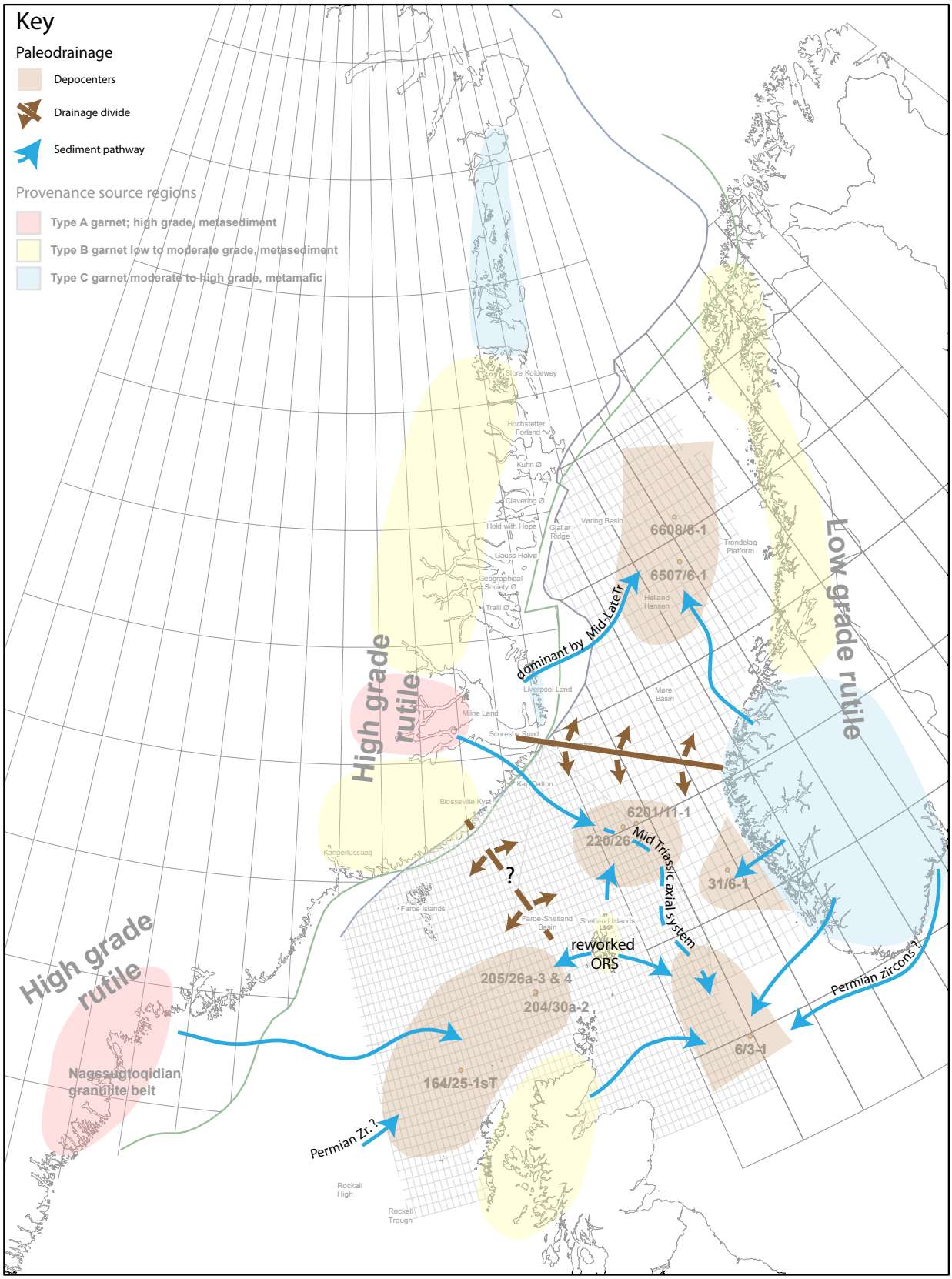

Figure 8. Illustration of the key characteristics of the proposed sediment sources and the inferred sediment pathways and paleodrainage for the North Atlantic region during the Triassic. Five main depocenters and a significant N-S drainage divide are identified. The establishment of a larger axial system resulted in sediment from East Greenland reaching the southern Viking Graben by the mid Triassic. Provenance characteristics are tied back to source regions using information from Kalsbeek et al. (1984, 1993), Sørensen and Kalvig (2002), van Gool et al. (2002), Morton et al. (2004, 2008, 2009b, 2012), Morton and Chenery (2009), Bingen and Solli (2009), and Thrane and Keulen (2015). ORS—Old Red Sandstone.

Northern Margin of the Shetland Platform and Southernmost Møre Basin

Combined heavy-mineral, single-grain geochemistry and zircon age data indicate that the entire succession in well 220/26-2 was derived from a broadly similar source, but there is evidence for a change in character from base to top. Garnet and rutile data indicate the source terrain was dominated by high-grade metasedimentary rocks, including abundant Type A garnets, with an overall increase in metamorphic grade with time (Figs. 5 and 6). There is also evidence for a subtle change in lithology, with metapelitic rocks becoming more dominant with time. These changes may also account for the observed increase in RuZi and MZi and the decrease in epidote content. Apatite roundness data indicate the lower part of the succession underwent more prolonged transport than the upper part. Zircon data indicate that early Paleozoic granitoids were an important component of the source region, with supply from such rocks increasing with time, mainly at the expense of the broad mid-Proterozoic group. The origin of the major Archean group (present throughout) and the wide-ranging mid-Proterozoic zircons (common in the older sample but poorly represented at the top) is uncertain, since it is unclear if these are first-cycle or recycled from metasediments associated with the Caledonian fold belt.

A likely source for the succession is the local northern part of the Shetland Platform given the proximity of this region (Fig. 8). The influx of fresh unrounded apatite and coincident increase in MZi, together with the increase in high-grade metapelitic detritus, decrease in apatite roundness, and changes in the zircon spectra, marks the introduction of sediment with a different character, possibly related to an increase in run-off due to more humid climatic conditions. A similar explanation has been proposed to account for coincident changes in mineral morphology and provenance character of the Triassic in the central North Sea (Mange-Rajetzky, 1995; McKie and Audretsch, 2005; McKie et al., 2010).

East Greenland and Norway are alternative sources for the detritus. The Milne Land–Renland region of East Greenland is interpreted as the source of the Åre Formation in the Heidrun Field, which has high-grade metasedimentary provenance characteristics (Morton et al., 2009a), including abundant Type A garnets, similar to those in well 220/26-2. However, the relatively large proportion of Archean zircons in well 220/26-2 is not mirrored in the Heidrun Field (Morton et al., 2009a), which argues against derivation from the same part of East Greenland. Derivation from Norway can be unequivocally ruled out on the basis of garnet geochemistry and the abundance of Archean zircons.

Provenance constraints on the uncored section in the adjacent well 6201/11-1 are less well established owing to poor sample quality, but the available data suggest there is little difference between the cored and uncored sections. With the exception of the topmost core sample, the core has similar provenance characteristics to those associated with the upper part of 220/26-2, and a similar northern Shetland Platform source is considered most likely. Garnet compositions in the topmost sample indicate a change to a lower-grade metamorphic source, but at this stage, there is no additional information (such as zircon age data and rutile compositions) to help establish the location of the candidate source area.

Northeastern North Sea

The Triassic in well 31/6-1, located in the northeastern part of the northern North Sea adjacent to the Norwegian landmass, has uniform provenance character throughout, as shown by the lack of significant variation in conventional heavy-mineral and garnet geochemical data (Figs. 4 and 5). The garnet assemblages, which are dominated by the high-Ca, high-Mg (Type C) component, are diagnostic of input from the adjacent parts of western Norway, including the Western Gneiss Region (Morton et al., 2004). Further support for derivation from western Norway is given by the predominantly metamafic nature of the rutile assemblages and the zircon spectrum dominated by grains formed during the Sveconorwegian (ca. 1000 Ma) orogenic event (Bingen et al., 2008) that overprinted the earlier Gothian event in this region (Beyer et al., 2012).

The only difference in heavy-mineral character in the succession occurs at the very top, at the transition from the Hegre Group to the Statfjord Formation. At this level, assemblages change from being epidote-dominated to epidote-poor, accompanied by decreasing ATi and GZi. However, garnet compositions show no change across the boundary, which suggests that the observed differences in heavy-mineral assemblages result from increased weathering rather than from any major change in source. A similar decrease in apatite and garnet is evident at the base of the Statfjord Group elsewhere in the northern North Sea (for example, the Snorre Field), where it has been attributed to a combination of increased weathering and changes in source (Mearns et al., 1989; Morton and Hurst, 1995).

Southern Viking Graben

Norwegian well 6/3-1, located in the southern part of the Viking Graben, displays a distinct change in provenance character approximately mid-way through the Skaggerak Formation. The upper part of the succession comprises sandstones with low-moderate grade metamorphic assemblages, exemplified by Type B garnets and amphibolite-facies rutiles. Zircon age data indicate input from a range of crustal sources with peaks corresponding to the Caledonian orogenic cycle (ca. 400–480 Ma), the Sveconorwegian orogeny (ca. 1000 Ma), Telemarkian magmatism (ca. 1500 Ma), and the Gothian orogeny (ca. 1650 Ma), all of which can be matched with a southwestern Scandinavian provenance (Bingen and Solli, 2009). The origin of the small group of Archean zircons, which form 4%–10% of the populations, is less clear, since zircons of this age are scarce in the basement in southern Norway and sediments in the Caledonian Nappe Domain (Morton et al., 2008; Bingen and Solli, 2009; Beyer et al., 2012). The most likely explanation is that they were derived from the source

that dominated the lower part of the succession, either through continued but much reduced supply, or through reworking.

The older part of the Skagerrak Formation has features that indicate greater input from high-grade metasediments, notably abundant Type A garnet and granulite-facies rutile. These features indicate affinities either with the Milne Land–Renland region of East Greenland (which supplied the Åre Formation in Heidrun and, as discussed below, the equivalent on the Nordland Ridge), or with the northern Shetland Platform, which is interpreted as the predominant source of sandstones in wells 220/26-2 and 6201/11-1. The zircon spectrum is more closely comparable with that of the Milne Land–Renland region, since Archean and early Paleozoic zircons are less abundant than in wells 220/26-2 and 6201/11-1. However, it is important to note that the zircon data from the lower part of the Skagerrak are from a ditch cuttings sample and may be contaminated with detritus from a higher stratigraphic level. This sample also has a small group of Permian zircons similar to those present in larger numbers on the western margin of the British Isles. It is considered most likely that the sandstones in the lower part of the Skagerrak Formation in well 6/3-1 has an along-axis supply from the north, either from the East Greenland area or the northern Shetland Platform (Fig. 8), supplemented by material sourced from southwestern Scandinavia; this source material became dominant in the upper part of the succession.

Nordland Ridge

The Triassic succession (including the Åre Formation) on the Nordland Ridge shows evidence for differences in sourcing between the three main sand packages. The uppermost unit, the Åre Formation and the "Grey Beds," has heavy-mineral assemblages, garnet geochemistry, and zircon age distributions directly comparable to the equivalent Åre Formation in the Heidrun Field on the Halten Terrace to the south (Fig. 1) for which the source was traced back to the Milne Land–Renland region in East Greenland by Morton et al. (2009a) (Fig. 8).

The middle package ("Red Beds") contains high-grade metasedimentary detritus similar to that forming the Åre Formation, implying sourcing from East Greenland. However, rutile assemblages indicate additional involvement of lower-grade metamorphic rocks including both metamafic and metapelitic lithologies, and the zircon spectrum indicates increased supply from rocks dated as ca. 1000 Ma and ca. 1500–1700 Ma. A similar provenance is seen in the short section analyzed from 6608/8-1. These data suggest that East Greenland sediment was augmented by detritus sourced from western Norway (Fig. 8).

The lower package in 6507/6-1 (Wordie Creek Formation equivalent) was derived from a generally rutile-poor source, with garnet data indicating considerable heterogeneity in composition. Lower-grade (Type B) garnets are most common, but Types A and C grains are also present. The zircons are closely comparable to those in the middle package, and dual sourcing from East Greenland and western Norway is considered likely. However, the origin of the additional small Permian group of zircons, similar in age to those found farther to the south, remains uncertain.

Permian Zircons

Permian (strictly speaking, latest Carboniferous to early Triassic) zircons have been found in a number of locations in the study area. They are most abundant in the northern Rockall Trough and west of Shetland area, but are also found in the southern Viking Graben and in the Nordland Ridge. They are also observed in the Triassic of the Corrib Field, west of Ireland (Franklin et al., 2019), where they range from 313 Ma (latest Carboniferous) to 243 Ma (Anisian) (Fig. 9). They are most common in the 290–300 Ma range, with younger grains tending to progressively decrease in abundance (Fig. 9). Nevertheless, in most areas, there is representation across the full Permian age range. The zircons on the Nordland Ridge, however, appear to be younger than those farther south, with no grains older than ca. 262 Ma having been identified in this area. Those from the southern Viking Graben form the oldest population

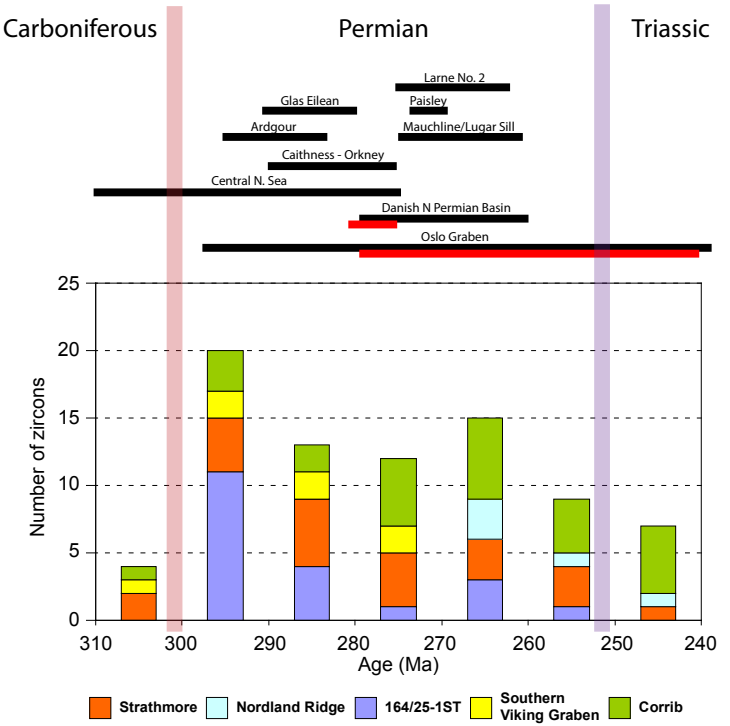

Figure 9. Age ranges of Permian zircons from the studied wells compared to the age of volcanics from the region (black = basic; red = acidic). Although the magmatic rocks are largely basic, and therefore unlikely to source abundant zircons, it is shown that magmatic activity at this time was widespread, and in some instances, acidic intrusives and extrusives are recorded. Age ranges of magmatic rocks are compiled from Sundvoll et al. (1990), Stemmerik et al. (2000), Glennie (2002), and Heeremans et al. (2004).

(310–270 Ma). There is no clear relationship between the presence of Permian zircons and the heavy-mineral character of the sands in which they are found.

The origin of these Permian zircons is unclear. It is unlikely that they could have been derived from the British margin, since magmatic rocks of this age are comparatively scarce and generally have basaltic or lamprophyric compositions (Fig. 9) that are unlikely to yield significant volumes of zircon. Furthermore, where garnet compositions suggest a more significant sediment input from the UK landmass (such as the Otter Bank Formation), Permian zircons are absent (Figs. 5 and 7).

The more likely possibilities are (1) that the zircons are related to rifting along the NE Atlantic margin, or (2) that they were supplied from the Arctic, where magmatism was associated with the Uralian orogeny followed by extrusion of the Siberian Traps. The distribution of the zircons suggests an Arctic origin is unlikely, except perhaps for the zircons on the Nordland Ridge, which are younger and possibly unrelated to the occurrences farther south.

If the end-Carboniferous intracontinental rifting along the line of the Rockall Trough, the Faroe-Shetland Basin, and the Norwegian-Greenland Sea proposed by Smythe et al. (1995) was associated with magmatism, it is possible that this could have generated the zircons now found in the Triassic. As outlined above, magmatic rocks of broadly consistent ages to the zircon age ranges reported here are described widely from across the west of the UK, the central North Sea, and into the Oslo Graben (Fig. 9), apart from the earliest Triassic ages, which are absent aside from a K/Ar age of 250 Ma from the Orkney dike swarm (Baxter and Mitchell, 1984). These rocks are predominantly basic in composition and therefore have low zircon fertility. However, the Danish North Permian Basin (Stemmerik et al., 2000) and the Oslo Graben (Sundvoll et al., 1990) do include significant acidic components. Given the widespread nature of the magmatic rocks of this age in the west of the UK, similar rift-related basic and acidic magmatism to that recorded in the Oslo Graben may be expected in the offshore and therefore provide a source for the Permian zircons recorded in the Corrib, northern Rockall Trough, and Strathmore regions. The Permian zircons recognized in the south Viking Graben may have originated locally from magmatism related to the Oslo Graben.

Position of Drainage Divides

Drainage from the North Atlantic region ultimately ended in the Boreal Ocean to the north and the Tethys Sea to the south, implying that a drainage divide must have existed between these two catchments. The data presented here provide evidence for the position of this major drainage divide during the Triassic. Sediments with a provenance signature consistent with East Greenland (Milne Land–Renland region), characterized by abundant Type A garnets, are found in both the Nordland Ridge region and at times as far south as 6/3-1 in the northern North Sea (Fig. 5). This suggests that the Milne Land–Renland source region straddles the drainage divide (Fig. 8). On the basis of the presented zircon data, a further potential drainage divide has been identified, separating the northern margin of the Shetland Platform from the Northern Rockall Trough and the southern Faroe-Shetland Basin. Further analysis would be required to provide confidence in the positioning of this second drainage divide.

As rifting proceeded through the Triassic, it seems probable that the associated drainage divides varied in their influence, and perhaps their exact position, but the evidence presented suggests sediment sourced from East Greenland was transported southward to the Viking Graben, and northward to the Boreal Ocean throughout the Triassic. It seems likely that the drainage divides were not defined by pronounced relief but rather displayed similarities to the subtle drainage divides described from the North Sea by McKie and Williams (2009). Ascertaining the structural controls on the positioning of the identified drainage divides is complex with Triassic features often overprinted by structures related to later phases of rifting. However, inherited Caledonian structures have been shown to exert a major influence on subsequent rifting throughout the North Atlantic (e.g., Fazlikhani et al., 2017) and therefore are considered below.

The NE-SW–oriented Triassic structural grain recognized in East Greenland and the Mid-Norway Margin (Guarnieri et al., 2017; Stoker et al., 2017) contrasts markedly with the N-S–oriented rift structures of the North Sea. The Møre-Trøndelag fault complex forms the boundary between these two domains. Undoubtably this zone of structural complexity would have had some effect on rifting during the Triassic and may have contributed to the development of the N-S watershed proposed here, potentially controlling a narrowing in the rift system and the development of associated topography. It should, however, be considered, that the Møre-Trøndelag fault complex runs northeastwards from Shetland to Norway and therefore must have been breached to allow drainage southwards from East Greenland.

A further large-scale tectonic feature that may have impacted rifting in the north Atlantic and therefore the position of the identified drainage divides is the Central Fjord structure and Flannan reflector. These features mirror the Caledonian front, which runs through western Scotland and then northwards through East Greenland and are interpreted to be underpinned by a fossil subduction zone (Schiffer et al. 2019). A series of highs depicted by Stoker et al. (2017), and inferred by McKie and Williams et al. (2009) to run between Shetland and Greenland's Blosseville Kyst, appears to follow this alignment and may therefore be an inherited expression of this underlying structural complexity. This would be consistent with the second drainage divide tentatively identified here to separate the northern margin of the Shetland Platform from the Northern Rockall Trough and the southern Faroe-Shetland Basin.

CONCLUSIONS

Major regional and stratigraphic variations in provenance are recorded across the Triassic of the North Atlantic regions. Five distinct provenance domains have been recognized: the northern Rockall Trough and southern Faroe-Shetland Basin; the northern margin of the Shetland Platform and southern Møre Basin; the northeastern part of the North Sea; the Viking Graben; and the Nordland Ridge (Fig. 8).

During the Early Triassic in the southern Faroe-Shetland Basin, significant reworking of local Old Red Sandstone is inferred. A distinct change is recognized in the Mid to Late Triassic with an influx of Type A garnets. In conjunction with zircon age spectra that include Permian, Paleoproterozoic (ca. 1900 Ma), and Archean (ca. 2700 Ma) peaks, and evidence for rutile of granulite facies origin, it is suggested that southern East Greenland (Fig. 8) acted as a significant sediment source to this region at this time. The origin of Permian zircons is most likely to be from rift-related magmatism along the NE Atlantic margin.

Triassic sandstones north of the Shetland Platform and in the southern Møre Basin have some provenance characteristics in common with sediment shed from the Milne Land–Renland region of East Greenland, particularly the abundance of Type A garnets and granulite-facies rutiles. However, a significant local input from the Shetland Platform seems likely in order to account for differences recognized in the zircon age spectra. It is notable that no Permian zircons are recorded in this region, and therefore transport of such zircons through this region seems unlikely.

One well was examined from the northeastern part of the North Sea (31/6-1). A uniform provenance character was recognized throughout, dominated by Type C garnets typical of sediment derived from the Western Gneiss Region, which lies directly east of this well (Fig. 8). Therefore, the Triassic in this region was locally sourced.

The Triassic of the southern Viking Graben contains evidence for a major shift in provenance during the mid-Triassic. The lower part of the Triassic succession in 6/3-1 is dominated by sandstones with a provenance affinity to the Milne Land–Renland or northern Shetland Platform regions. The affinity to a Milne Land–Renland source may provide evidence for a major southerly flowing axial transport system at this time (Fig. 8), perhaps reflecting a period of more humid conditions during the early to mid-Triassic. Furthermore, sediment being sourced from the Milne Land–Renland region would necessitate the drainage divide between systems flowing northwards to the Boreal Ocean, and those flowing southward to the Tethys sea, to lie adjacent to or northwards of the Milne Land–Renland source region (Fig. 8). Later in the Triassic, a switch to Norwegian-sourced sediment is recognized.

The Nordland Ridge has a thick Early to Late Triassic succession. Type A garnets are abundant throughout the succession suggesting a predominantly Greenland source (Fig. 8). Greenland sourced sediment was supplemented by sediment from western Norway, especially in the lower and middle parts of the succession. These inferred transport pathways further constrain the position of N-S drainage divide discussed above, and indicate that the Milne Land–Renland region must straddle this divide (Fig. 8).

Permian zircons are a common feature in the earliest Triassic sediments along the western margin of the British Isles. Their origin remains uncertain, but they are most likely associated with rift-related magmatism in the NE Atlantic. More work is required to understand the wider regional distribution and sourcing of these zircons.

The identification of sediment transport systems reaching >800 km, southwards from East Greenland to the south Viking Graben, has important implications for paleogeographic reconstructions of the region. Furthermore, it should condition our models of the fluvial systems we might expect and therefore the characteristics of potential reservoir targets in the subsurface.

The regional and stratigraphic trends presented here are made on the basis of a small number of wells, and a number of questions still exist. Increasing the well coverage and integrating these data with the equivalent onshore succession from East Greenland will provide a higher-resolution data set that will improve our understanding of sediment distribution patterns during the Triassic. Furthermore, the detailed data presented here can form a framework for heavy-mineral correlation throughout the region.

ACKNOWLEDGMENTS

The authors would like to thank the consortium of subscribing oil and gas companies for its financial support to the CASP Norway-Greenland Project. We are also grateful to BP for allowing release of provenance data acquired from Norwegian wells 6507/6-1 and 6608/8-1. Sophie Leleu and an anonymous reviewer are also thanked for their useful comments.

REFERENCES CITED

Andrews, S.D., Kelly, S.R.A., Braham, B., and Kaye, M., 2014, Climatic and eustatic controls on the development of a Late Triassic source rock in the Jameson Land Basin, East Greenland: Journal of the Geological Society of London, v. 171, no. 5, p. 609–619, https://doi.org/10.1144/jgs2013-075.

Baxter, A., and Mitchell, J., 1984, Camptonite-monchiquite dyke swarms of Northern Scotland; Age relationships and their implications: Scottish Journal of Geology, v. 20, p. 297–308, https://doi.org/10.1144/sjg20030297.

Beyer, E.E., Brueckner, H.K., Griffin, W.L., and O'Reilly, S.Y., 2012, Laurentian provenance of Archean mantle fragments in the Proterozoic Baltic crust of the Norwegian Caledonides: Journal of Petrology, v. 53, p. 1357–1383, https://doi.org/10.1093/petrology/egs019.

Bingen, B., and Solli, A., 2009, Geochronology of magmatism in the Caledonian and Sveconorwegian belts of Baltica: Synopsis for detrital zircon provenance studies: Norsk Geologisk Tidsskrift, v. 89, p. 267–290.

Bingen, B., Nordgulen, Ø., and Viola, G., 2008, A four-phase model for the Sveconorwegian orogeny, SW Scandinavia: Norsk Geologisk Tidsskrift, v. 88, p. 43–72.

Daly, J., Heaman, L., Fitzgerald, R., Menuge, J., Brewer, T., and Morton, A., 1995. Age and crustal evolution of crystalline basement in western Ireland and Rockall, *in* Croker, P.F., and Shannon, P.M., eds.,, The Petroleum Geology of Ireland's Offshore Basins: Geological Society of London Special Publication 93, p. 433–434, https://doi.org/10.1144/GSL.SP.1995.093.01.34.

Doré, A.G., 1992, Synoptic palaeogeography of the Northeast Atlantic Seaway: Late Permian to Cretaceous, *in* Parnell, J., ed., Basins on the Atlantic Seaboard: Petroleum Geology, Sedimentology and Basin Evolution: Geological Society of London Special Publication 62, p. 421–446, https://doi.org/10.1144/GSL.SP.1992.062.01.31.

Fazlikhani, H., Fossen, H., Gawthorpe, R.L., Faleide, J.I., and Bell, R.E., 2017, Basement structure and its influence on the structural configuration of the northern North Sea rift: Tectonics, v. 36, no. 6, p. 1151–1177, https://doi.org/10.1002/2017TC004514.

Fisher, M.J., and Mudge, D.C., 1998, Triassic, *in* Glennie, K.W., ed., Petroleum geology of the North Sea: Basic concepts and recent advances: Oxford, Blackwell Science, p. 212–244, https://doi.org/10.1002/9781444313413.ch7.

Franklin, J., Tyrrell, S., Morton, A., Frei, D., and Mark, C., 2019, Re-evaluating Triassic sand supply to the Slyne Basin, offshore western Ireland, applying a multi-proxy provenance approach: Journal of the Geological Society, v. 176, p. 1120–1135, https://doi.org/10.1144/jgs2019-085.

Frei, D., and Gerdes, A., 2009, Precise and accurate in-situ U-Pb dating of zircon with high sample throughput by automated LA-SF-ICP-MS: Chemical Geology, v. 261, p. 261–270, https://doi.org/10.1016/j.chemgeo.2008.07.025.

Galehouse, J.S., 1971, Point-counting, *in* Carver, R.E., ed., Procedures in Sedimentary Petrology: New York, Wiley-Interscience, p. 385–407.

Gerdes, A., and Zeh, A., 2006, Combined U-Pb and Hf isotope LA-(MC)-ICP-MS analyses of detrital zircons: Comparison with SHRIMP and new constraints for the provenance and age of an Armorican metasediment in Central Germany: Earth and Planetary Science Letters, v. 249, p. 47–61, https://doi.org/10.1016/j.epsl.2006.06.039.

Glennie, K.W., 2002, Permian and Triassic, *in* Trewin, N.H., ed., The Geology of Scotland (4th edition): The Geological Society of London, p. 213–249.

Goldsmith, P.J., Hudson, G., and Van Veen, P., 2003, Triassic, *in* Evans, D., Graham, C., Armour, A., and Bathurst, P., eds., The Millennium Atlas: Petroleum Geology of the Central and northern North Sea: Geological Society of London, p. 105–127.

Guarnieri, P., Brethes, A., and Rasmussen, T.M., 2017, Geometry and kinematics of the Triassic rift basin in Jameson Land (East Greenland): Tectonics, v. 36, no. 4, p. 602–614, https://doi.org/10.1002/2016TC004419.

Heeremans, M., Timmerman, M.J., Kirstein, L.A., and Faleide, J.I., 2004, New constraints on the timing of late Carboniferous–early Permian volcanism in the central North Sea: Geological Society of London, Special Publications, v. 223, no. 1, p. 177–193, https://doi.org/10.1144/GSL.SP.2004.223.01.08.

Jackson, S., Pearson, N., Griffin, W., and Belousova, E., 2004, The application of laser ablation–inductively coupled plasma–mass spectrometry to in situ U-Pb zircon geochronology: Chemical Geology, v. 211, p. 47–69, https://doi.org/10.1016/j.chemgeo.2004.06.017.

Jacobsen, V., and van Veen, P., 1984, The Triassic offshore Norway north of 62°N, *in* Spencer, A.M., Holter, E., Johnsen, S.O., Mork, A., Nysether, E., Songstad, P., and Spinnangr, A., eds., Petroleum Geology of the North European Margin: London, Graham and Trotman, p. 317–327, https://doi.org/10.1007/978-94-009-5626-1_23.

Jochum, K., and Nehring, F., 2006, BCR-2: GeoRem preferred values (11/2006): GeoRem, http://georem.mpch-mainz.gwdg.de).

Kalsbeek, F., Taylor, P.N., and Henriksen, N., 1984, Age of rocks, structures, and metamorphism in the Nagssugtoqidian mobile belt, West Greenland-field and Pb-isotope evidence: Canadian Journal of Earth Sciences, v. 21, p. 1126–1131, https://doi.org/10.1139/e84-117.

Kalsbeek, F., Austrheim, H., Bridgwater, D., Hansen, B.T., Pedersen, S., and Taylor, P.N., 1993, Geochronology of Archaean and Proterozoic events in the Ammassalik area, South-East Greenland, and comparisons with the Lewisian of Scotland and the Nagssugtoqidian of West Greenland: Precambrian Research, v. 62, p. 239–270, https://doi.org/10.1016/0301-9268(93)90024-V.

Leleu, S., Hartley, A.J., van Oosterhout, C., Kennan, L., Ruckwied, K., and Gerdes, K., 2016, Structural, stratigraphic and sedimentological characterisation of a wide rift system: The Triassic rift system of the Central Atlantic Domain: Earth-Science Reviews, v. 158, p. 89–124, https://doi.org/10.1016/j.earscirev.2016.03.008.

Lervik, K., 2006, Triassic lithostratigraphy of the northern North Sea Basin: Norsk Geologisk Tidsskrift, v. 86, p. 93–125.

Ludwig, K.R., 2003, Isoplot/Ex version 3.0: A geochronological toolkit for Microsoft Excel: Berkeley Geochronology Center, Special Publication, 4.

Mange, M.A., and Maurer, H.F.W., 1992, Heavy minerals in colour: London, Chapman and Hall, 147 p, https://doi.org/10.1007/978-94-011-2308-2.

Mange, M.A., and Morton, A.C., 2007, Geochemistry of heavy minerals, *in* Mange, M.A., and Wright, D.T., eds., Heavy Minerals in Use: Developments in Sedimentology, v. 58, p. 345–391, https://doi.org/10.1016/S0070-4571(07)580,13-1.

Mange-Rajetzky, M.A., 1995, Subdivision and correlation of monotonous sandstones sequences using high resolution heavy mineral analysis, a case study: The Triassic of the Central Graben, *in* Dunay, R.E., and Hailwood, E.A., eds., Non-Biostratigraphical Methods of Dating and Correlation: Geological Society of London Special Publication 89, p. 23–30, https://doi.org/10.1144/GSL.SP.1995.089.01.03.

Manspeizer, W., 1988, Triassic Jurassic Rifting: Continental Breakup and the Origin of the Atlantic Ocean and Passive Margins: Amsterdam, Elsevier Publishing Co., 998 p.

Mattinson, J., 2010, Analysis of the relative decay constants of 235U and 238U by multi-step CA-TIMS measurements of closed-system natural zircon samples: Chemical Geology, v. 275, p. 186–198, https://doi.org/10.1016/j.chemgeo.2010.05.007.

McClay, K.R., Norton, M.G., Coney, P., and Davis, G.H., 1986, Collapse of the Caledonian orogen and the Old Red Sandstone: Nature, v. 323, p. 147–149, https://doi.org/10.1038/323147a0.

McKie, T., 2014, Climatic and tectonic controls on Triassic dryland terminal fluvial system architecture, central North Sea, *in* Martinius, A.W., Ravnås, R., Howell, J.A. Steel, R.J. and Wonham, J.P., eds., Depositional Systems to Sedimentary Successions on the Norwegian Continental Margin. International Association of Sedimentologists, Special Publication, v. 46, p. 19–58.

McKie, T., and Audretsch, P., 2005, Depositional and structural controls on Triassic reservoir performance in the Heron Cluster, ETAP, Central North Sea, *in* Doré, A.G., and Vining, B.A., eds., Petroleum Geology: North-West Europe and Global Perspectives—Proceedings of the 6th Petroleum Geology Conference: Geological Society of London, p. 285–298.

McKie, T., and Williams, B., 2009, Triassic palaeogeography and fluvial dispersal across the northwest European Basins: Geological Journal, v. 44, p. 711–741, https://doi.org/10.1002/gj.1201.

McKie, T., Jolley, S., and Kristensen, M., 2010, Stratigraphic and structural compartmentalization of dryland fluvial reservoirs: Triassic Heron Cluster, Central North Sea, *in* Jolley, S.J., Fisher, Q.J., Ainsworth, R.B., Vrolijk, P.J., and Delisle, S., eds., Reservoir Compartmentalization: Geological Society of London Special Publication 347, p. 165–198, https://doi.org/10.1144/SP347.11.

Mearns, E., Knarud, R., Raestad, N., Stanley, K.T., and Stockbridge, C., 1989, Samarium-neodymium isotope stratigraphy of the Lunde and Statfjord formations of Snorre oil field, northern North Sea: Journal of the Geological Society of London, v. 146, p. 217–228, https://doi.org/10.1144/gsjgs.146.2.0217.

Meinhold, G., 2010, Rutile and its applications in earth sciences: Earth-Science Reviews, v. 102, p. 1–28, https://doi.org/10.1016/j.earscirev.2010.06.001.

Meinhold, G., Anders, B., Kostopoulos, D., and Reischmann, T., 2008, Rutile chemistry and thermometry as provenance indicator: An example from Chios Island, Greece: Sedimentary Geology, v. 203, p. 98–111, https://doi.org/10.1016/j.sedgeo.2007.11.004.

Morton, A., and Chenery, S., 2009, Detrital rutile geochemistry and thermometry as guides to provenance of Jurassic–Paleocene sandstones of the Norwegian Sea: Journal of Sedimentary Research, v. 79, p. 540–553, https://doi.org/10.2110/jsr.2009.054.

Morton, A., and Hurst, A., 1995, Correlation of sandstones using heavy minerals: an example from the Statfjord Formation of the Snorre Field, northern North Sea, *in* Dunay, R.E., and Hailwood, E., eds., Dating and Correlating Biostratigraphically-Barren Strata: Geological Society of London Special Publication 89, p. 3–22, https://doi.org/10.1144/GSL.SP.1995.089.01.02.

Morton, A., Hallsworth, C., and Chalton, B., 2004, Garnet compositions in Scottish and Norwegian basement terrains: a framework for interpretation of North Sea sandstone provenance: Marine and Petroleum Geology, v. 21, p. 393–410, https://doi.org/10.1016/j.marpetgeo.2004.01.001.

Morton, A., Fanning, M., and Milner, P., 2008, Provenance characteristics of Scandinavian basement terrains: Constraints from detrital zircon ages in modern river sediments: Sedimentary Geology, v. 210, p. 61–85, https://doi.org/10.1016/j.sedgeo.2008.07.001.

Morton, A., Hallsworth, C., Strogen, D., Whitham, A., and Fanning, M., 2009a, Evolution of provenance in the NE Atlantic rift: the Early–Middle Jurassic succession in the Heidrun Field, Halten Terrace, offshore mid-Norway: Marine and Petroleum Geology, v. 26, p. 1100–1117, https://doi.org/10.1016/j.marpetgeo.2008.07.006.

Morton, A., Hallsworth, C., Kunka, J., Laws, E., Payne, S., and Walder, D., 2010, Heavy mineral stratigraphy of the Clair Group (Devonian-Carboniferous) in the Clair Field, west of Shetland, UK, *in* Ratcliffe, K.T., and Zaitlin, B.A., eds., Application of Modern Stratigraphic Techniques: Theory and Case Histories: Society for Sedimentary Geology (SEPM) Special Publication v. 94, p. 183–199.

Morton, A., Ellis, D., Fanning, M., Jolley, D., and Whitham, A., 2012, The importance of an integrated approach to provenance studies: A case study from the Paleocene of the Faroe-Shetland Basin, NE Atlantic, *in* Rasbury, E.T., Hemming, S.R., and Riggs, N.R., eds., Mineralogical and Geochemical Approaches to Provenance: Geological Society of America Special Paper 487, p. 1–12, https://doi.org/10.1130/2012.2487(01).

Morton, A., Frei, D., Stoker, M., and Ellis, D., 2014, Detrital zircon age constraints on basement history on the margins of the northern Rockall Basin, *in* Cannon, S., and Ellis, D., eds., Exploration and Exploitation West of Shetlands: Geological Society of London Special Publication 397, p. 209–223, https://doi.org/10.1144/SP397.12.

Morton, A.C., 1985, A new approach to provenance studies: electron microprobe analysis of detrital garnets from Middle Jurassic sandstones of the northern North Sea: Sedimentology, v. 32, p. 553–566, https://doi.org/10.1111/j.1365-3091.1985.tb00470.x.

Morton, A.C., and Hallsworth, C.R., 1994, Identifying provenance specific-features of detrital heavy mineral assemblages in sandstones: Sedimentary Geology, v. 90, p. 241–256, https://doi.org/10.1016/0037-0738(94)90041-8.

Morton, A.C., and Hallsworth, C.R., 2007, Stability of detrital heavy minerals during burial diagenesis, *in* Mange, M.A., and Wright, D.T., eds., Heavy Minerals in Use: Developments in Sedimentology, v. 58, p. 215–245, https://doi.org/10.1016/S0070-4571(07)58007-6.

Morton, A.C., Herries, R., and Fanning, M., 2007, Correlation of Triassic sandstones in the Strathmore Field, west of Shetland, using heavy mineral provenance signatures, *in* Mange, M.A., and

Wright, D.T., eds., Heavy Minerals in Use: Developments in Sedimentology, v. 58, p. 1037–1072, https://doi.org/10.1016/S0070-4571(07)58041-6.

Morton, A.C., Hitchen, K., Fanning, C.M., Yaxley, G., Johnson, H., and Ritchie, J.D., 2009b, Detrital zircon age constraints on the provenance of sandstones on Hatton Bank and Edoras Bank, NE Atlantic: Journal of the Geological Society of London, v. 166, p. 137–146, https://doi.org/10.1144/0016-76492007-179.

Mouritzen, C., Farris, M.A., Morton, A., and Matthews, S., 2017, Integrated Triassic stratigraphy of the greater Culzean area, UK central North Sea: Petroleum Geoscience, v. 24, p. 197–207, https://doi.org/10.1144/petgeo2017-039.

Müller, R., Nystuen, J.P., Eide, F., and Lie, H., 2005, Late Permian to Triassic basin infill history and palaeogeography of the Mid-Norwegian shelf–East Greenland region: Onshore-Offshore Relationships on the North Atlantic Margin: Norwegian Petroleum Society Special Publication, v. 12, p. 165–189, https://doi.org/10.1016/S0928-8937(05)80048-7.

Nasdala, L., Hofmeister, W., Norberg, N., Mattinson, J., Corfu, F., Dörr, W., Kamo, S., Kennedy, A., Kronz, A., Reiners, P., Frei, D., Košler, J., Wan, Y., Götze, J., Häger, T., Kröner, A., and Valley, J., 2008, Zircon M257—A homogeneous natural reference material for the ion microprobe U-Pb analysis of zircon: Geostandards and Geoanalytical Research, v. 32, p. 247–265, https://doi.org/10.1111/j.1751-908X.2008.00914.x.

Pearce, N.J., Perkins, W.T., Westgate, J.A., Gorton, M.P., Jackson, S.E., Neal, C.R., and Chenery, S.P., 1997, A compilation of new and published major and trace element data for NIST SRM 610 and NIST SRM 612 glass reference materials: Geostandards newsletter, v. 21, no. 1, p.115–144.

Price, S.P., Brodie, J.A., Whitham, A.G., and Kent, R., 1997, Mid-Tertiary rifting and magmatism in the Traill Ø region, East Greenland: Journal of the Geological Society of London, v. 154, p. 419–434, https://doi.org/10.1144/gsjgs.154.3.0419.

Scanlon, R., and Daly, J., 2001, Basement architecture of the rifted Northeast Atlantic margin: Evidence from a combined geochronology, fission-track and potential field study: Boston, Massachusetts, Geological Society of America Annual Meeting, Abstracts with Programs, paper 64-0.

Schiffer, C., Peace, A., Phethean, J., Gernigon, L., McCaffrey, K., Petersen, K.D., and Foulger, G., 2019, The Jan Mayen microplate complex and the Wilson cycle, *in* Wilson, R.W., Houseman, G.A., McCaffrey, K.J.W., Doré, A.G., and Buiter, S.J.H., eds., Fifty Years of the Wilson Cycle Concept in Plate Tectonics: Geological Society of London Special Publication 470, no. 1, p. 393–414.

Schmidt, A., Morton, A., Nichols, G., and Fanning, C., 2012, Interplay of proximal and distal sources in Devonian–Carboniferous sandstones of the Clair Basin, west of Shetland, revealed by detrital zircon U-Pb ages: Journal of the Geological Society of London, v. 169, p. 691–702, https://doi.org/10.1144/jgs2011-148.

Sircombe, K., 2004, AgeDisplay: An EXCEL workbook to evaluate and display univariate geochronological data using binned frequency histograms and probability density distributions: Computers & Geosciences, v. 30, p. 21–31, https://doi.org/10.1016/j.cageo.2003.09.006.

Sláma, J., Košler, J., Condon, D., Crowley, J., Gerdes, A., Hanchar, J., Horstwood, M., Morris, G., Nasdala, L., Norberg, N., Schaltegger, U., Schoene, B., Tubrett, M., and Whitehouse, M., 2008, Plešovice zircon—A new natural reference material for U-Pb and Hf isotopic microanalysis: Chemical Geology, v. 249, p. 1–35, https://doi.org/10.1016/j.chemgeo.2007.11.005.

Smythe, D.K., Russell, M.J., and Skuce, A.G., 1995, Intra-continental rifting inferred from the major late Carboniferous quartz-dolerite dyke swarm of NW Europe: Scottish Journal of Geology, v. 31, p. 151–162, https://doi.org/10.1144/sjg31020151.

Sørensen, J.B., and Kalvig, P., 2002, Garnet sand in Greenland: Examples from Tuttoqqortooq, Tasiilaq area and Sisimiut area: Danmarks og Grønlands Geologiske Undersøgelse Rapport 2002/12.

Stacey, J.S., and Kramers, J.D., 1975, Approximation of terrestrial lead isotope evolution by a two-stage model: Earth and Planetary Science Letters, v. 26, p. 207–221, https://doi.org/10.1016/0012-821X(75)90088-6.

Stemmerik, L., Vigran, J.O., and Piasecki, S., 1991, Dating of late Paleozoic rifting events in the North Atlantic: New biostratigraphic data from the uppermost Devonian and Carboniferous of East Greenland: Geology, v. 19, p. 218–221, https://doi.org/10.1130/0091-7613(1991)019<0218:DOLPRE>2.3.CO;2.

Stemmerik, L., Ineson, J., and Mitchell, J., 2000, Stratigraphy of the Rotliegend Group in the Danish part of the northern Permian Basin, North Sea: Journal of the Geological Society of London, v. 157, p. 1127–1136, https://doi.org/10.1144/jgs.157.6.1127.

Stoker, M.S., Stewart, M.A., Shannon, P.M., Bjerager, M., Nielsen, T., Blischke, A., Hjelstuen, B.O., Gaina, C., McDermott, K., and Ólavsdóttir, J., 2017, An overview of the Upper Palaeozoic–Mesozoic stratigraphy of the NE Atlantic region: Geological Society of London Special Publications, v. 447, no. 1, p. 11–68, https://doi.org/10.1144/SP447.2.

Sundvoll, B., Neumann, E.-R., Larsen, B., and Tuen, E., 1990, Age relations among Oslo Rift magmatic rocks: Implications for tectonic and magmatic modelling: Tectonophysics, v. 178, p. 67–87, https://doi.org/10.1016/0040-1951(90)90460-P.

Surlyk, F., 1990, Timing, style and sedimentary evolution of Late Palaeozoic–Mesozoic extensional basins of East Greenland, *in* Hardman, R.P.F., and Brooks, J., eds., Tectonic Events Responsible for Britain's Oil and Gas Reserves: Geological Society of London Special Publication 55, p. 107–125, https://doi.org/10.1144/GSL.SP.1990.055.01.05.

Surlyk, F., Hurst, J.M., Piasecki, S., Rolle, F., Scholle, P.A., Stemmerik, L., and Thomsen, E., 1986, The Permian of the western margin of the Greenland Sea—A future exploration target, *in* Halbouty, M.T., ed., Future Petroleum Provinces of the WorldAmerican Association of Petroleum Geologists Memoir 40, p. 629–659.

Swiecicki, T., Wilcockson, P., Canham, A., Whelan, G., and Homann, H., 1995, Dating, correlation and stratigraphy of the Triassic sediments in the West Shetlands area, *in* Boldy, S.A.R., ed., Permian and Triassic Rifting in Northwest Europe: Geological Society of London Special Publication 91, p. 57–85, https://doi.org/10.1144/GSL.SP.1995.091.01.04.

Thrane, K., and Keulen, N., 2015, Provenance of sediments in the Faroe–Shetland Basin: Characterisation of possible source components in Southeast Greenland. 5th Faroe Islands Exploration Conference: Proceedings of the 4th Conference, p. 7–25.

Tyrrell, S., Leleu, S., Souders, A.K., Haughton, P.D., and Daly, J.S., 2009, K-feldspar sand-grain provenance in the Triassic, west of Shetland: distinguishing first-cycle and recycled sediment sources?: Geological Journal, v. 44, p. 692–710, https://doi.org/10.1002/gj.1185.

van Gool, J.A., Connelly, J.N., Marker, M., and Mengel, F.C., 2002, The Nagssugtoqidian Orogen of West Greenland: Tectonic evolution and regional correlations from a West Greenland perspective: Canadian Journal of Earth Sciences, v. 39, p. 665–686, https://doi.org/10.1139/e02-027.

Watson, E.B., Wark, D.A., and Thomas, J.B., 2006, Crystallization thermometers for zircon and rutile: Contributions to Mineralogy and Petrology, v. 151, p. 413–433, https://doi.org/10.1007/s00410-006-0068-5.

Whitham, A.G., Price, S.P., Koraini, A.M., and Kelly, S.R.A., 1999, Cretaceous (post-Valanginian) sedimentation and rift events in the NE Greenland (71°–77°N), *in* Fleet, A., and Boldy, S., eds., Petroleum Geology of Northwest Europe: Proceedings of the 5th Conference: Geological Society of London, p. 325–336.

Wiedenbeck, M., Alle, P., Corfu, F., Griffin, W.L., Meier, M., Oberli, F., Von Quadt, A., Roddick, W., and Speigel, W., 1995, Three natural zircon standards for U-Th-Pb, Lu-Hf, trace-element and REE analyses: Geostandards Newsletter, v. 19, p. 1–23, https://doi.org/10.1111/j.1751-908X.1995.tb00147.x.